CHAPTER 1

INTRODUCTION

This Section briefly describes the background to the project described in this thesis. Electrometallurgy is the last process for the recovery, and therefore production of copper metal from the mining industry. Copper electrometallurgy includes electrorefining and electrowinning depending on whether the copper mineral was processed through pyrometallurgy or hydrometallurgy. A 2003 world survey[1, 2] indicated that the production of electrolytic copper was about 13,066 kilotonnes per year of which about 2,375 kilotonnes per year proceeded from electrowinning operations.

Recent advances in hydrometallurgy led Mount Gordon Operations of Western Metals Copper Ltd., Australia to treat some copper sulphide ores directly in an autoclave reactor. Mount Gordon Operations (Mt. Gordon) was the first hydrometallurgical plant in the Western World to produce copper cathode using a mild-pressure autoclave ferric ion-sulfuric acid leach[3, 4]. The Mt. Gordon flowsheet is depicted in Figure 1-1. Initially, the feed to the plant was chalcocite ore, but later, it was a semi-concentrate with about 12 percent copper content. Mt. Gordon had occasionally produced the smoothest copper cathode ever known in the industry and also experienced premature detachment of the copper cathode from the stainless steel substrate, known as “pre-stripping” in the industry.

Nonionic polyacrylamide (MW 15 million Dalton, Magnafloc® 800HP, approx. theoretical length 10-50μm) from Ciba was dosed as flocculant to the hydroclassifiers and pinned bed clarifiers. It was highly likely that occasionally polyacrylamide (PAM) passed through the solvent extraction stage and then reached the electrowinning plant where it may have acted as an organic additive. Thus, the electrolyte contained two organic additives: Guarfloc66 (Guar), the industry-standard organic additive and PAM. These organic additives may have *occasionally* assisted to Mt. Gordon into the production of *highly smooth* copper cathodes. However, it was unclear, at this time, whether this smoothness was the effect of polyacrylamide by itself or its combination with Guar. The smoothness of the copper cathode led to the development of this thesis to study polyacrylamide as an organic additive for copper electrowinning.

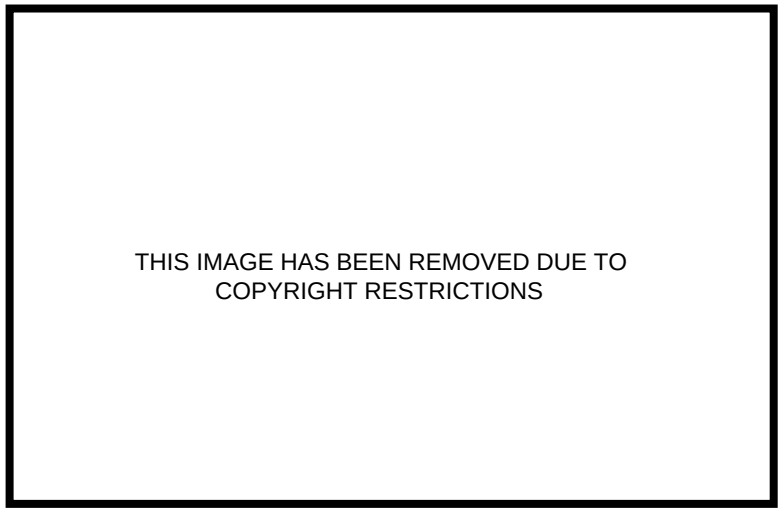

Figure 1-1: Mount Gordon Operations Flowsheet[4, 5]

1.1 Problem Statement

It is widely recognized that the initial process of electrochemical crystal growth and subsequent formation of monolayers are affected by the crystallographic properties of the substrate and metal deposit itself. It is therefore necessary to use additives to control nucleation and growth during the deposition process. These additives enable the production of smooth copper deposits free of voids and porosity. Such copper deposits also routinely achieve a higher level of polycrystalinity and ductility. In the absence of additives, the morphology of the copper deposit will be columnar, containing large crystals which enhance dendrite growth. Such morphology is counter-productive to achieving a high quality copper cathode and plant productivity.

The recent literature has widely discussed the advances in copper electrodeposition for the damascene process in the fabrication of interconnects (IC) and printed circuit boards (PCB). These studies consistently indicate that a levelling agent (often also called an inhibitor), an accelerator (also often called a grain refiner in electrometallurgy) and chloride ions should be dosed to produce "superconformal" growth. It is also known that animal glue, a leveller; thiourea (a grain refiner) and chloride ions have been dosed in copper electrorefining for more than 100 years. However, only guar gum (Guar) and chloride ions have been dosed in copper *electrowinning* for the last 40 years. Guar is known as a weak levelling agent in the industry. Table 1-1 briefly summarizes these industry-standard additives used in copper electrodeposition and their typical concentrations and their respective roles.

Research and development on the effects of Guar (often also known as a "weak polarizer" and/or "brightener" within the industry) and chloride ions in copper electrowinning has been neglected, notwithstanding that about 20% of the copper cathodes produced around the World comes from electrowinning operations. It appears that the mature technology of copper electrometallurgy knows only glue as a levelling agent throughout the World. It is a concern within the industry that additives other than Guar may affect the components of the organic solvent extractant (LIX®984 or ACORGA®M5640 and kerosene type diluent). Moreover, it also appears to be an understanding in the industry that the highly purified copper electrolyte after solvent

extraction does not require a levelling agent and grain refiner. However, commercial laboratories for the fabrication of PCB and IC not only use reagent grade copper sulfate and sulfuric acid but also a levelling agent. Surfactants such as PEG and a grain refiner or accelerator are used to obtain void-free "superfilling" or "superconformal" growth of nanometer scale trenches and vias.

Table 1-1: Industry-Standard Additives Used in Copper Electrodeposition

Role of the Additive	Electrorefining		Electrowinning		Microelectronics, PCB and IC	
	Additive	mg/L	Additive	mg/L	Additive	mg/L
Leveller	glue	1	Nil	Nil	PEG*	100-300
Brightener**			Guar	0.25-5		
Grain refiner	thiourea	2	Nil	Nil	SPS&JGB/MPSA*	1&1/1, respectively
Depolarizer	Cl^-	50-60	Cl^-	20-25	Cl^-	40-60

*PEG, polyethylene glycol; SPS, bis(3-sulfo-propyl) disulfide; JGB, Janus Green B (safranine dye); MPSA, 3-mercapto-1-propanesulfinate. **Guar is also known as weak polarizer in the industry.

The polarizer/inhibitor/leveller controls the vertical growth to produce smooth deposits by conferring preferential adsorption on the peaks or active sites. The grain refiner/accelerator may predominantly control the nucleation process or promote the formation of new nuclei to possibly form new crystallites at the recesses. This synergistic process between the inhibitor and grain refiner is aimed at improving the overall quality of the copper deposit: purity, smoothness and plant productivity i.e., elimination/reduction of short-circuits caused by dendrites

1.2 Thesis Objectives

The aim of this thesis project is to compare and understand the fundamental events at the solid-electrolyte interface during the electrodeposition of copper in the presence of Guar and a *new* organic additive developed in this thesis. This thesis will characterise and compare Guar and the newly developed organic additive in terms of their roles as levelling agents and/or grain refiners during the deposition process.

A smooth copper cathode improves the plant productivity in terms of current efficiency. It may also assist to increase the current density and the purity of the copper cathode by reducing entrainment of solid particles. A London Metal Exchange Grade "A" copper (less than 0.0065% total impurities excluding O, C, and H) attracts

premium. This thesis also attempts to bring together and apply the knowledge gained on copper deposition for the fabrication of PCB and IC with the experience gained from the mature industry of copper electrometallurgy.

CHAPTER 2

LITERATURE REVIEW

2.1 Electrodeposition Process Fundamentals

Electrodeposition is the formation of a new solid phase on a substrate immersed in an ionic conducting electrolyte under the influence of an electric field [6-10]. The electrolyte generally consists of an electro-active species and a supporting electrolyte to improve its conductivity. The overall reaction process involves the following individual steps[7]:

(i) Mass transfer of the reactants from the bulk solution to the electrode/electrolyte interface via diffusion and convection,

(ii) Formation of metal adatoms, M_{ads}, on a same-metal substrate, M, or on foreign substrate, S, via adsorption and transfer of electrons from the cathode to the reactant,

(iii) Two-dimensional (2D) and three-dimensional (3D) metal phase formation via nucleation and growth.

In the following sections, the convective diffusion equation is developed for strong electrolyte solutions such as a cupric ions-sulfuric acid electrolyte to develop a physicochemical model. The mass transfer for cupric ions based on the equation

developed for the rotating cylinder electrode is also discussed to show the importance of the type of the supporting electrolyte such as sulfuric acid.

2.2 Transport Processes in Electrolytic Solutions

A review of the overall experimental/laboratory based literature on electrodeposition of metals shows that a rotating disc electrode (RDE) has been more often used than a rotating cylinder electrode (RCE). However, copper electrorefining and electrowinning at commercial scale takes place in parallel plate electrodes where a uniform current distribution is prevalent since the insulator forms an angle close to 90^o (right angle) with the electrode[10]. As the primary and mass-transfer-limited current distribution are more uniform on a RCE than a RDE[10, 11]; Newman[10] suggests that perhaps more attention should be devoted to the possibility of using a RCE rather than RDE. This problem with the RDE becomes more serious for fast reactions and large current densities[10].

The hydrodynamics for the RDE[10] are well understood possibly due to its critical Reynolds number[12] of 10^5 and it is therefore most often used in the laminar regime, i.e., 300-500rpm. The critical Reynolds number for the RCE is about 200[12] and therefore turbulent flow is achieved at low speeds of rotation. However, the ohmic potential drop and concentration change at the electrode can be accurately calculated even in turbulent flow when the RCE is used[10]. Therefore, the RCE may be the preferred electrochemical cell to study copper deposition at 300-400A/m^2 to measure and quantify the effect of additives due to its uniform current distribution. Moreover, the hydrodynamics in commercial copper electrowinning may also be simulated more closely using a RCE than RDE.

2.2.1 Mass Transfer

Step (*i*) in Section 2.1, mass transfer, is governed by the hydrodynamic transport law for dilute solutions and can also be generalized for strong solutions to express the molar flux (mole/s) of an ionic species[10]. The flux density N_i of a species *i* is equal to its velocity multiplied by its concentration.

$$N_i = -z_i u_i F c_i \nabla\Phi - D_i \nabla c_i + c_i v_i \qquad (2\text{-}1)$$

The first term on the RHS of Equation 2-1 represents the flux due to electric field migration where z_i is the charge number of the ion, u_i its mobility, F the Faraday constant, c_i concentration of species i, and $\nabla\Phi$ the electric field. The second term represents the diffusion flux due to a concentration gradient: the species will diffuse from regions of high concentration to regions of low concentration, and the third term represents the convection flux due to motion of the solution with bulk velocity, ν.

The transient material balance is given by:

$$\frac{\partial c_i}{\partial t} = -\nabla \cdot N_i + R_i \qquad (2\text{-}2)$$

where the term on the LHS is the accumulation rate, the first term on the RHS is the net input differential volume element and R_i is the production (in homogeneous chemical reactions) in mol/cm^3.s. The differential volume element is simply the time rate of concentration change. In electrochemical systems, the reaction is frequently restricted to electrode surfaces, in which case R_i is zero. As the solution is also electrically neutral except in a thin double charge layer near the electrode and other boundaries, it is reasonable to adopt Equation 2-3 in the context of the electroneutrality of the bulk solution.

$$\sum_i z_i c_i = 0 \qquad (2\text{-}3)$$

In the presence of a supporting electrolyte such as sulfuric acid and due to the incompressibility of the electrolyte ($\nabla\cdot\nu = 0$), the flux Equation 2-1 above can be combined with Equation 2-2 to produce Equation 2-4. The supporting electrolyte is frequently added to increase the conductivity of the solution and thereby reduce the electric field.

$$\frac{\partial c}{\partial t} + \nu\nabla c_i = z_i F \nabla(u_i c_i \nabla\Phi) + \nabla(D_i \nabla c_i) + R_i \qquad (2\text{-}4)$$

Equation 2-4 can be used to determine the concentration distribution when the fluid velocity and potential distributions are known. A further simplification of Equation 2-4 can be applied when migration is neglected and the requirement of electroneutrality allows the potential to be eliminated[10, 13]. Thus, the mass transfer is primarily due to diffusion and convection, therefore the concentration distribution is governed by the known *convective diffusion*, Equation 2-5 for a constant diffusion coefficient[10] and strong electrolyte solutions.

$$\frac{\partial c_i}{\partial t} + v \cdot \nabla c_i = D_i \nabla^2 c_i \qquad (2\text{-}5)$$

where

c_i is the concentration of species i, mol/cm^3

v is the mass-average velocity, cm/s

D_i is the diffusion coefficient of species i, cm^2/s

Equation 2-5 can be used to develop a physicochemical model for copper electrodeposition.

2.3 Rotating Cylinder Electrodes

The mass transfer of reactants from the bulk solution to the electrode/electrolyte interface via diffusion and convection stated in Equation 2-5 for the overall reaction process will be discussed using the hydrodynamic properties of the RCE. Although the turbulent flow cannot yet be fully analyzed from fundamental principles; the rotating cylinder electrode has been studied and analysed by many authors[10, 14-18]. The RCE was selected for this thesis to approximate the fluid flow of the electrolyte during commercial scale copper electrowinning[19].

If the cathodic current density is much less than the limiting, mass transfer controlled current density, for a cathodic reaction, neglecting the reverse, oxidation reaction, the limiting diffusion current density, i_L is given by Fick's first law, Equation 2-6, with a surface concentration of zero[20].

$$i_L \equiv \frac{nFDC_b}{\delta} \qquad (2\text{-}6)$$

where δ, cm, is the diffusion layer thickness.

Mass transfer between concentric cylinders, the inner of which is rotating with an angular speed ω has been studied[10, 14, 16]. The limiting current density for the RCE is described as follows according to Eisenberg et al.[14].

$$i_L = 0.0791\frac{nFDC_b}{di}(\mathrm{Re})^{0.7}(Sc)^{0.356} \qquad (2\text{-}7)$$

where

i_L is the limiting current density, mA/cm^2,

n is the number of electrons transferred in the electrode reaction,

F, Faraday's constant, 96,487C/equivalent and,

D, diffusion coefficient of electrolyte, cm^2/s,

C_b is copper concentration in the bulk solution, mol/cm^3,

di is the diameter of the inner, rotating cylinder, cm,

Re is the Reynolds number, ($\omega d^2/2\nu$),

ω is the rotation speed in rad/s,

ν is the kinematic viscosity, cm^2/s,

Sc is the dimensionless Schmidt number, (ν/D)

Equating Equations 2-6 and 2-7, the Nernst diffusion model for the RCE can be expressed as[14]:

$$\delta = 12.64\frac{di^{0.30}\nu^{0.344}D^{0.356}}{U^{0.70}} \qquad (2\text{-}8)$$

Eisenberg et al.[14] developed the empirical Equation 2-7 using the hexacyanoferrate (II) and hexacyanoferrate (III) in 2M NaOH as supporting electrolyte at 25^{o}C.

Arvia et al[15] also developed an equation for the RCE, Equation 2-9, using 1.5-3.5 g/L cupric ions in 1.5M sulfuric acid at 18°C. The experimental RCE of Arvia et al.[15] had the inner, rotating electrode as anode and a fixed cathode as the outer electrode. This experimental set up was opposite to that of Eisenberg et al.[14] and to the experimental set up for this thesis. The limiting current density for the RCE can also be calculated using the equation developed by Arvia et al[15]. The difference between Equations 2-7 and 2-9 possibly reflect the effect of sulfuric acid in Arvia et al[15] experiments.

$$i_L = 0.0791\, nFC_b \left(\frac{di}{\nu}\right)^{-0.30} (U)^{0.70} \left(\frac{do}{di}\right) (Sc)^{-0.644} \qquad (2\text{-}9)$$

where U is the peripheral velocity, *di* and *do* are the inner, rotating and outer-static cylinders diameters, respectively. The other variables are described as above.

The addition of sulfuric acid as supporting electrolyte in copper electrodeposition has several effects on the behaviour of the system. First, the conductivity is increased; thereby reducing the electric field in solution for a given current density and, second, the transference number of the cupric ion is reduced[10]. Therefore, the role of migration in the transport of cupric ion and the ohmic potential drop in solution are greatly reduced; the importance of diffusion in the transport of cupric ion is increased[10]. Since migration is reduced, the supporting electrolyte decreases the limiting current density. The conductivity of 6.3 g/L cupric ions will increase from 0.00872S/cm to 0.548S/cm when 150g/L H_2SO_4 is added to the copper electrolyte but the limiting current density will decrease from 79mA/cm^2 using the equation developed by Eisenberg et al.[14] to 48mA/cm^2 using a RCE at 900rpm[10]. If the concentration of cupric ions is increased from 6.3 to 44.5g/L in 150g/L sulfuric acid, the conductivity still will be about 0.0375S/cm.

The rotation of one electrode in the RCE electrochemical cell can produce flow patterns that assist in reducing the concentration gradient and contribute to the transport of materials to the electrode surface. Very low rotation speeds lead to simple laminar flow in concentric circles in which the fluid velocity is perpendicular to the direction of

mass transfer. This simple flow pattern becomes unstable at higher rotation speeds, particularly if the inner electrode rotates and Taylor vortices or laminar flow with vortices can be obtained resulting in an enhanced mass transfer[10]. Moreover, in the laminar flow Taylor vortices region, there is a radial and axial motion, inward at one point and outward at different axial position superimposed to the tangential motion. At higher rotation speeds, the flow becomes turbulent with Taylor vortex flow[21] with further enhancement of the mass transfer. Wang[21] recently studied the Taylor-Couette flow and indicated the disappearance and reappearance of azimuthal waves depending on the ratio of the Reynolds number to the Reynolds critical number.

The fluid flow at rotating cylinder electrodes can be described using the Reynolds and Taylor numbers. Reynolds number, Re has been expressed differently in the literature if $d_{Rotating}$=di, Re=U*d/ν =ω*ri*di/ν > Re= ω*di^2/ν > Re=ω*di^2/2ν = U*di/ν where ω is the rotation speed, rad/s, *di* is the inner rotating diameter, *ri* is the inner rotating radius, d is radius of the outer cylinder minus radius of the inner cylinder (ro-ri) and U is the peripheral velocity in cm/s. The first equality was used by Schlichting[22] and Wang et al.[21], respectively. The second equation was used by Silverman[23]. The third equality was used by Newman[10], Gabe[12], Eisenberg et al.[14] and Arvia et al.[15]. These Reynolds numbers are slightly different as shown in Appendix A. This difference is due to the selection of the radius, diameter and/or inter-electrode distance as the characteristic length for the rotating cylinder electrode.

The predominance of Taylor vortices is given by the Taylor number [Ta, Ta= (U*d/ν*√d/ri)][22, 23]. However, this Taylor number appears to be only valid for small inter-electrode gap, e.g. 0.19cm, and the Taylor vortices may vary from 41.3 to 400. For larger electrode gaps, e.g., 3.2cm, such as is used in this thesis, the fluid flow at the RCE appears to be most often described by the Reynolds number (Re = ω*di^2/2ν), and the Taylor number, Ta = [(Re^2)(d/ri)]. Newman in 1973[24] defined that turbulent flow prevails for Reynolds numbers greater than 3960 or Taylor numbers greater than about $3x10^6$. Using the above Reynolds equation described above, the critical Reynolds number for a RCE is 200[12].

At currents below, but at a significant fraction of the limiting current, it is necessary to calculate the concentration variations near the electrode. The surface concentration can be calculated using the following equation[10]:

$$\frac{i_n}{i_L} = 1 - \frac{C_o}{C_b} \qquad (2\text{-}10)$$

and if Equation 2-6 is inserted in Equation 2-10, the surface concentration of cupric ions is given by Equation 2-11 to develop a physicochemical model:

$$C_o = C_b - \delta \frac{i_n}{2DF} \qquad (2\text{-}11)$$

where

C_o is the surface concentration at the electrode surface, mol/cm^3,
C_b is the bulk concentration of cupric ions, mol/cm^3,
δ is the diffusion layer thickness, cm,
i_n is the normal current density at electrode surface, A/cm^2,
D is the diffusion coefficient of cupric ions, cm^2/s,
F is the Faraday's constant, 96,487, C/equiv.

The equations developed by Eisenberg et al.[14] and Arvia et al.[15] will be compared with the experimental data produced in this thesis. Computational fluid dynamics of the electrolyte fluid flow around the electrode during copper electrowinning indicate that the hydrodynamic boundary layer varies between 250 and 300 μm[19].

2.4 Electrochemical Kinetics Fundamentals

The first task of electrode kinetics is to explain the sequence of partial reactions constituting the overall electrode reaction or reaction mechanism and the second task is the determination of electrode reaction rates or the application of Faraday's law[6]. The dependence of current density, the reaction rate, on the electrode potential, the

concentration of reactants and other variables such as temperature and transport processes must also be determined.

In summary, the analysis of the behaviour of electrochemical systems seeks to formulate the relationship between the current density and electrode potential, surface overpotential, and the composition adjacent to the electrode surface as well as the temperature.

Copper dissolution and deposition are widely regarded as being composed of two elementary steps, each of which involves the transfer of an electron:

$$\begin{array}{lcll} & & & E^o(V) \\ & k_1 & & \\ Cu^{2+} + e^- & \rightleftharpoons & Cu^+_{(ads)} \quad \text{(slow)} & 0.159^{25} \qquad (2\text{-}12) \\ & k_{-1} & & \\ & k_2 & & \\ Cu^+_{(ads)} + e^- & \rightleftharpoons & Cu^o \quad \text{(fast)} & 0.520^{25} \qquad (2\text{-}13) \\ & k_{-2} & & \end{array}$$

The first reduction step is much slower than the second step.[10, 26] Mattsson and Bockris[26] studied the deposition and dissolution of copper in acid sulfate electrolyte by a galvanostatic technique and found that the overall reaction obeys the Butler-Volmer equation, Equation 2-14. This equation is valid irrespective of the presence and absence of additives and it is related to surface overpotential, η_s; F, Faraday's constant; i_n, the normal component of the faradic current density which is related to the normal component of the flux of cupric ions and, i_o, exchange current density. The number of electrons transferred is n.

$$i_n = i_o[\exp(\frac{\alpha_a F}{RT}\eta_s) - \exp(-\frac{\alpha_c F}{RT}\eta_s)] \qquad (2\text{-}14)$$

α_a and α_c are two additional kinetic parameters termed as the *transfer coefficients* and the theoretical values are 1.5 and 0.5, respectively and their sum, $\alpha_a + \alpha_c$, equal to 2[10, 26]. The symmetry factor β_3 ($\alpha_a = 2-\beta_3$ and $\alpha_c = \beta_3$) for Equation 2-14 is

equal to 0.5[26]. Newman[10] further examined Mattsson and Bockris[26] data and suggested that β_3 in the exponent of composition dependence of the exchange current density, γ, ($\gamma = (2-\beta_3)/2$) has a value 0.42 rather than 0.50. It is therefore ascertained that the exchange-current density, i_o depends strongly on the composition at the interface[10] as

$$i_o = \left(\frac{c_{Cu^{2+}}}{Cu^{\infty}_{Cu^{2+}}} \right)^{\gamma} i_o\left(c^{\infty}_{Cu^{2+}}\right).$$

The probability for simultaneous electron transfer in a single step is extremely low since the time scale for an electron transfer event, ca. 10^{-16} s is much smaller than the time scale of the fastest chemical reorganization in the metal-ligand vibration scale, 10^{-13} s or slower[27]. The rate constants k_1 and k_2 have been explained to have different kinetics with $i_{o,1}$ and α_1 and $i_{o,2}$ and α_2, characterising each process, respectively. The general expression for a sequential two-electron reaction derived by Vetter[6, 27] is:

$$i = -2i_{o,1} \exp(-\frac{(1-\alpha_1)}{RT} F\eta) \times \frac{1-\exp(\frac{2F}{RT}\eta)}{1+(\frac{i_{o,1}}{i_{o,2}})\exp[\frac{(1+\alpha_1-\alpha_2)}{RT}F\eta]} \qquad (2\text{-}15)$$

where η=E-E^o and E^o is the standard electrode potential for the overall two-electron process. The two rate-limiting cases are described below:

1. The first electron-transfer step is the rate determining step ($k_2 \gg k_{-1}$).The forward rate coefficient is $k_f \approx k_1$ and the backward rate coefficient is $k_b \approx \left(\frac{k_2}{k_{-2}} \right) / k_{-1}$.
2. The second electron-transfer step is the rate determining step ($k_2 \ll k_{-1}$) then $k_f \approx \left(\frac{k_1}{k_{-1}} \right) k_2$ and $k_b \approx k_{-2}$.

The first limiting case was demonstrated to be the rate determining step in copper electrodeposition in the presence of a supporting electrolyte[10, 26].

2.5 Effect of Additives on Copper Electrocrystallization

2.5.1 Introduction

The process of electrochemical crystal growth cannot be achieved under "ideal" conditions, i.e., without additives, due to the crystallographic properties of the substrate and depositing metal. In the copper deposition industry in general, chloride ions and organic additives need to be dosed to produce smooth deposits, free of voids or porosity and as a result its morphology can be changed and, polycrystalinity and highly ductility can also be achieved. It has been widely acknowledged that organic additives significantly influence the current-potential relationship due to their interactions for surface coverage with the components of the electrolyte system including with chloride ions. These interactions take place since some species in solution may have a preference for being near the solid.

Electrocrystallization denotes formation of new nuclei and crystal growth in electrochemical systems under the influence of an electric field. Nucleation is a very important process; the first step of metal-deposition is the formation of nuclei of the depositing metal on a foreign substrate or on a substrate of the same metal. The competition between nucleation and growth determine the smoothness of the deposit: higher nucleation rates yield smaller crystallite sizes[7].

On the other hand, the forms of the growing crystals determine the physical appearance and structure of the depositing metal. Thus a high growth rate of the crystal size normal to the substrate yields (*i*) a more fibrous or columnar microstructure and (*ii*) a brightening effect is achieved from large developed crystal faces parallel to the substrate. Therefore, the kinetics of nucleation and growth play a dominant role in determining the overall deposition kinetics, as well as the appearance, structure and properties of the deposit.

The literature on copper deposition in the presence of additives indicates that the type of adsorption onto the metal substrate is critical in affecting the deposition process. The whole array of charged species and oriented dipoles existing at the metal-electrolyte interface is called the *electrical double-layer* as described in Figure 2-2.

Figure 2-2 indicates that some components of the electrolyte bath are more closely adsorbed at the electrode interface, i.e., within the inner and outer Helmholtz planes (IHP and OHP) than other components. The electrolyte component more closely adsorbed is defined to be more *specifically adsorbed* and the component less closely adsorbed is defined to be *non-specifically adsorbed*[9, 10].

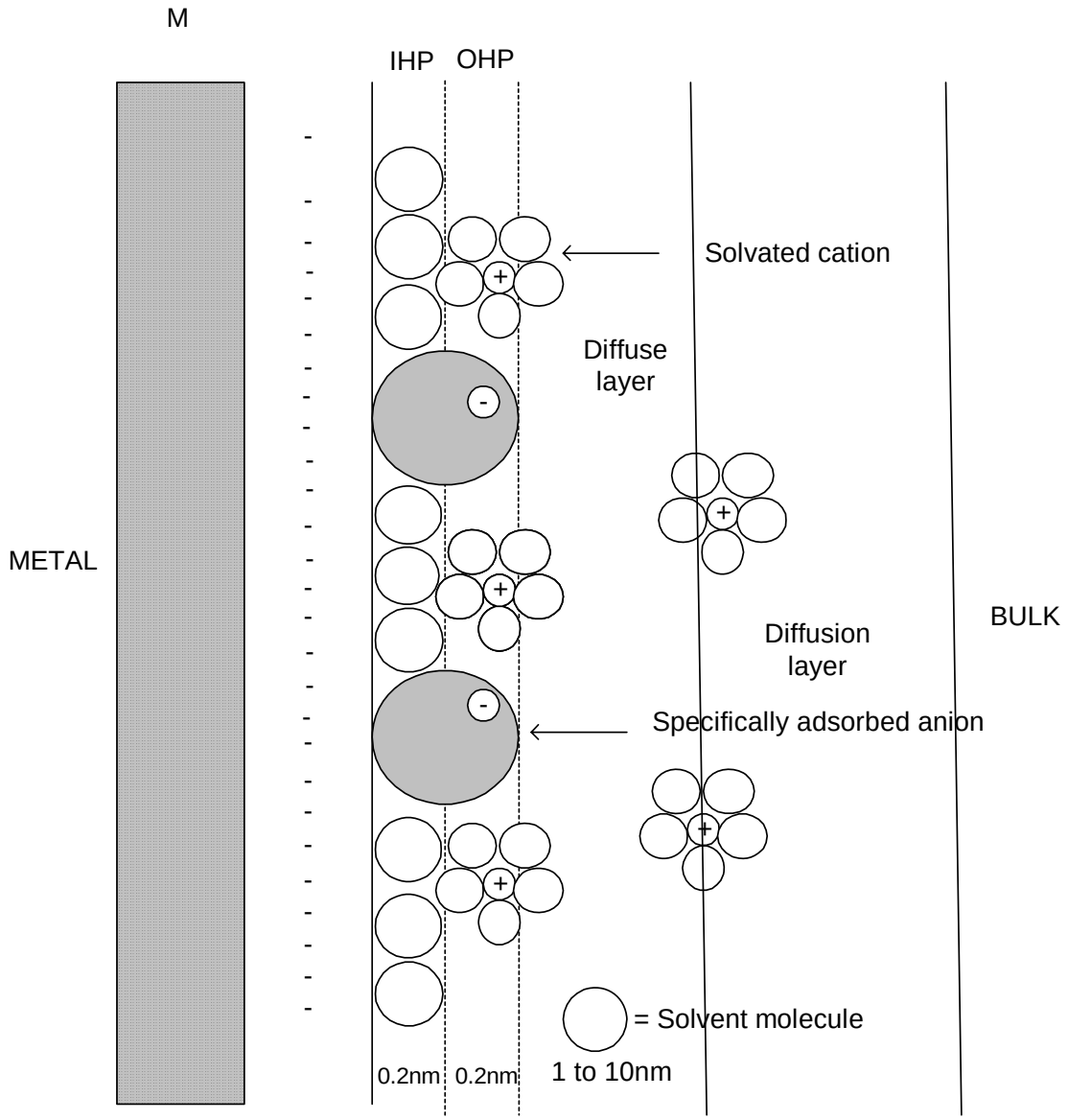

Figure 2-2: Schematic representation of the structure of the double-layer in electrolyte solution during electrochemical reactions where anions are specifically adsorbed.

The indicative dimensions of the IHP, OHP and diffuse layer represent mercury electrode[10]. Specifically adsorbed ions or molecules are located at the IHP while solvated adsorbed ions are located beyond (but not quite at) the OHP[9, 10].

2.5.2 Effect of Chloride Ions on Nucleation and Growth

The use of additives in copper electrodeposition is extremely important owing mainly to effects produced on the growth and microstructure such as brightening of the deposit, reducing crystallite size, reducing the tendency to grow dendrites, increasing the current density range, and changing the mechanical and physical properties and reducing stress[28].

Sun and O'Keefe[29] and Zhou and O'Keefe[30] studied the nucleation and growth of copper on stainless steel substrates using 40g/L Cu^{2+} and 180g/L H_2SO_4 at 40°C in the presence and absence of chloride ions, respectively. Sun and O'Keefe[29] found that irrespective of the presence or absence of chloride ions on a 304 stainless steel RDE seems to promote *progressive* nucleation, 3-D growth and diffusion control at various rotation speeds (0-1600rpm). In contrast, Zhou and O'Keefe[30] found that in the absence of chloride ion the copper nucleation mechanism on 316L substrate plate (as-received) appears to be *instantaneous* and diffusion controlled. It is therefore concluded that the initial nucleation and growth mechanism on stainless steel is not clear possibly due to the non-uniform current distribution of the RDE. Moreover, Sun and O'Keefe[29] also reported that in the presence of 40 mg/L chloride ions:

(i) the current density was 30 percent higher at a fixed potential than in the absence of chloride ions. This effect is defined as the *depolarizing* effect of an additive - in this case of chloride ions.

(ii) a decreasing number of nuclei and an enhanced redistribution of copper crystals was observed, that is coalescence of small crystals towards large crystals possibly due to binding[8] and surface energy differences[31] between the copper metal and stainless steel,

(iii) Secondary nucleation takes place preferably on already formed copper crystals rather than on the stainless steel substrate possibly due to the crystallographic misfit[8], and

(iv) The secondary nucleation leaves large portions of the stainless steel uncovered, and produces lacy copper or discontinuous deposits possibly due to surface diffusion[7].

Ilgar and O'Keefe[32] also studied the effect of chloride ions and indicated that it increased the surface roughness of the copper deposit. Chloride ions strongly adsorb on the surface of the cathode and the reduction of Cu^{+} to Cu becomes the rate limiting step instead of the reduction of Cu^{2+} to cuprous ion[33, 34]. A recent study also indicates that chloride ion is a depolarizer[35]. It can be seen that these independent studies agree to conclude that chloride ions have a *depolarizing* effect leading to non-uniform discontinuous deposits and higher levels of contained impurities[29].

2.5.3 Effect of Organic Additives on Nucleation and Growth

Copper deposition in the presence of polyethylene glycol (PEG), chloride ions, Janus Green B (JGB) and bis-(3-sulfopropyl) disulfide (SPS) in the electrolyte bath increased the progressive nucleation rate and nucleus density but the Volmer-Weber, Figure 2-3(a), growth mode was unchanged on n-Si(111) substrate[36]. It is widely known[7] that the growth mode depends on the binding energy (ψ) of adsorbed metal ions, M_{ads} on the substrate, S compared to that of M_{ads} on same M substrate and on the crystallographic misfit given by the inter-atomic distances $d_{o,M}$ and $d_{o,S}$ of 3D M and S bulk phases, respectively. The Volmer-Weber growth mode shown in Figure 2-3(a) indicates (3D M island formation) for ψM_{ads}-S « ψM_{ads}-M, independent of the ratio $(d_{o,M} - d_{o,S})/d_{o,S}$).

An ideal levelling agent and grain refiner at their correct concentrations including those of chloride ions can start the deposition process on 316L stainless steel with the Volmer-Weber and/or Stranski-Krastanov growth modes, Figures 2-3(a) and 2-3(c), respectively. These Figures show 3D M (metal) island formation prevail due to the crystallographic misfit given by inter-atomic distances between the depositing metal and the substrate and their binding energy differences. However, after about 20 monolayers of the depositing metal where the effect of the substrate on the depositing metal ceases[7] the Frank-van der Merwe growth mode, shown in Figure 2-3(b), where a layer-by-layer growth form prevails, is obtained.

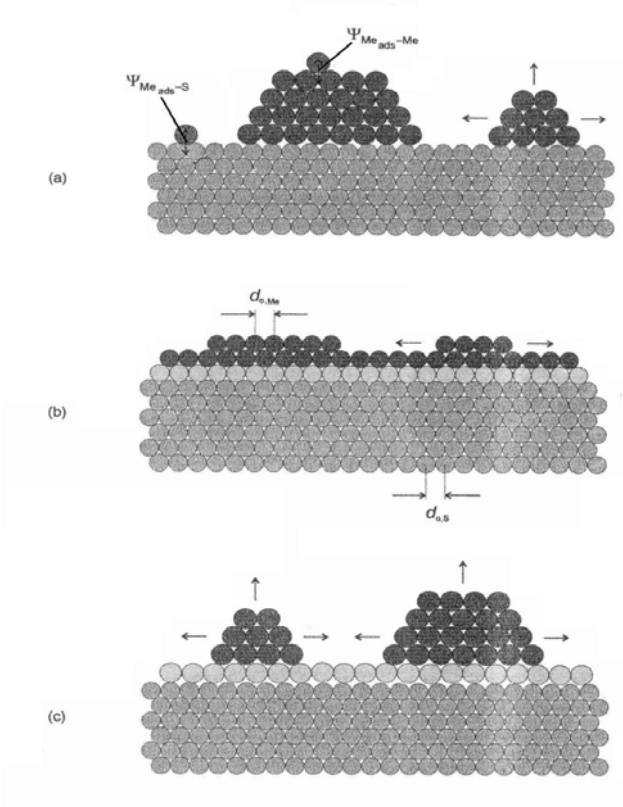

Figure 2-3: Schematic Representation of Different Growth Modes in Metal Deposition on Foreign Substrates.

(a) Volmer-Weber; (b) Frank-van der Merwe and (c) Stranski-Krastanov[7].

Deposition of copper on highly oriented pyrolytic graphite from additive-free solutions lead to rough surface textures due to diffusion limited 3D nucleation and growth. The addition of benzotriazole, a levelling agent, to the above bath inhibited the vertical growth and the lateral growth was charge-transfer limited. This process smoothes the deposit by diminishing surface diffusion[37].

It appears that there is also an overall consensus in the literature that the grain refiner/accelerator plays an important role in electrorefining and in the microelectronics industry. This role was recently described using atomic force microscopy and indicated that surface roughness of copper deposits obtained from PEG + SPS and chloride ions are nearly one-third those grown from SPS + chloride alone[38]. The PEG + SPS and Cl^- system also produces smaller features than the SPS + Cl^- alone. This effect of SPS appears to be a result of its interaction with Cl^-.

Thiourea [$(H_2N)_2C=S$] in copper *electrorefining* acts as grain refiner. Surface-enhanced Raman Scattering (SERS) spectroscopy indicates that sulfur atoms of thiourea and sulfate ions, but not bi-sulfate ions, cooperate rather than compete to bond onto copper atoms possibly at the most active sites[39]. This process possibly increases the number of new nuclei where new metal could grow or in other terms increases the rate of nucleation.

It has been shown in this Section that the presence of chloride ions and organic additives can change the nucleation and growth mode of copper deposition. It has been also shown that a levelling agent and a grain refiner/accelerator are dosed with chloride ions during copper deposition in electrorefining and in the microelectronics industry.

2.5.4 Copper Electrowinning in the Presence of Organic Additives

An extensive literature review revealed very few publications related to organic additives in copper *electrowinning* even though the industry is about 40 years old. In the first publication, Pye and Schurz (1957)[40] patented the electrowinning of zinc and copper in the presence of acrylamide polymer (homopolymer and copolymers of acrylamide). It was claimed that acrylamide polymer can be dissolved in *water* or *electrolyte* or may be added in a solid form to the copper electrolyte. The concentration of the acrylamide polymer in the electrolyte was claimed to vary from 25 to 150 mg/L to accomplish an improved deposition of the metal of concern. This patent also claims that the electrolyte contains 20-70 grams/L copper with a substantial proportion of sulfuric acid and it is essentially *free of chloride ions* to obtain smooth bright copper deposits after 5, 13 and 16 hours of electrowinning at 25^{o}C and 172 A/m^2 current density.

In a second publication, Vereecken and Winand (1976)[41] compared the influence of nonionic and cationic polyacrylamides with Guar Gum (Guar) on the quality of copper deposits using "industrial" copper sulphate solution at 200 Amp/m^2 and 50^{o}C. The electrolyte composition was (g/L): copper, 50; Mn, 10; Mg, 4; Co, 1.5; phosphate ions, 10 and sulfuric acid, 50. it should be noted that chloride ions were not reported to be present in the electrolyte and the sulfuric acid concentration is lower than that in

current plant practice. Moreover, it is unclear in the publication whether the nonionic and cationic polyacrylamides were prepared in water or in a solution of pH 3. Every 12 hours, 1mg/L of PAM was dosed for 48 hours of electrowinning. The conclusion of this study was that the quality of the copper deposits obtained with Guar was always better than those obtained with both nonionic and cationic polyacrylamides. It is stated by Vereecken that "the polarization curve was recorded for the reduction of Cu^{2+} ions on copper cathode with 1mg/l of the *different inhibitors*. This low concentration does not significantly change the overpotential of the cathode reduction. This confirms the results obtained during the electrolysis: the cathodic galvanic potential in all the experiments was equal to *+200mV/NHE* (the cell voltage was about 2V)". Vereecken and Winand[41] observed the depolarization behaviour of nonionic and cationic polyacrylamides, and Guar prepared in water or in a solution of pH 3.

The "active" concentration of Glue[42] and Guarfloc66[43], the industry-industry organic additives dosed in copper electrorefining and electrowinning, respectively were measured using CollaMat™. This technique determines the rate of polarization change by measuring the potential over short-time periods on platinum wire (diameter: ~1mm) correlated with the inhibitor concentration. It concluded that Guar activity was about 70 percent lower than Glue activity under the same conditions and indicated that Guar is a weak levelling agent.

2.5.5 Physicochemical Properties of Guar

Guar gum (Guar) is a naturally occurring galactomannan polymer, a polysaccharide, used as flocculant and coagulant with typical molecular weights ranging from $2x10^5$ to $5x10^5$ Dalton. Guar is a linear D-mannose sugar with a D-galactose sugar chain on every other mannose as shown below (Figure 2-5)[44].

Very little information was found on Guar hydrolysis and adsorption other than to say that it forms colloidal dispersions when hydrated in cold water[44]. No information was found on its adsorption mechanism on stainless steel or copper or any other substrate.

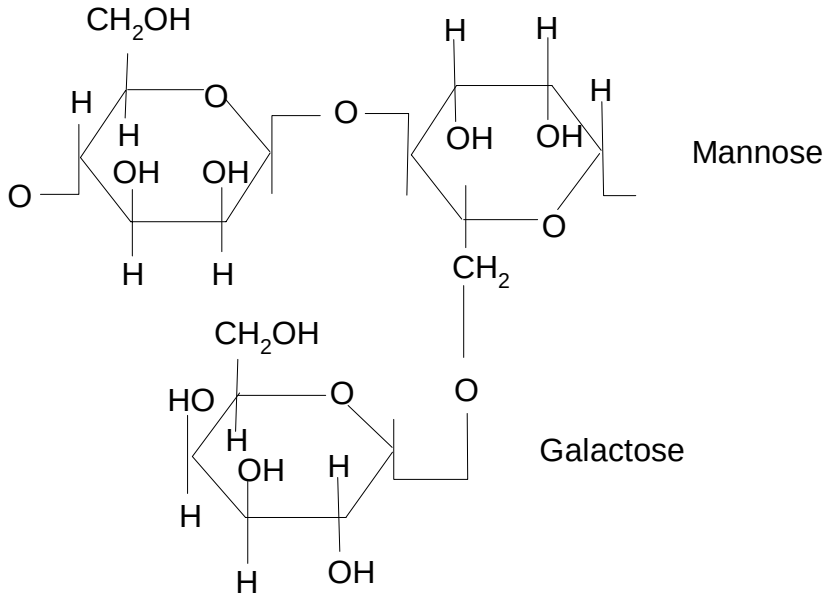

Figure 2-4: The chemical structure of Guar[44]

2.6 Polyacrylamide Hydrolysis and Adsorption

2.6.1 Introduction

(iv) This section presents an overview of the literature on polyacrylamide hydrolysis reactions and its molecular adsorption at electrified and non-electrified solid surfaces. Recent developments in surface electrochemistry explore the phenomena at the electrified solid-liquid interface by a combination of electrochemical, spectroscopic, diffraction and surface imaging techniques[45]. The knowledge gained from these studies is relevant to copper electrometallurgy, to study the coordination at electrode surfaces. The adsorption of an organic additive is a sought-after occurrence in copper electrometallurgy to produce smooth, void-free and low porosity copper deposits[29, 46, 47]. Smoothness assists to increase the purity of the copper deposit by reduction of particle and electrolyte entrainment, and results in an increase in plant productivity. In this thesis, the use of polyacrylamide as an organic additive is investigated.

Polyacrylamide is highly soluble in water but its solution viscosity limits its concentration to very low values, nevertheless among other polymers, it has a unique position for industrial applications due to its adsorption properties[48]. In general, the rheological behaviour of aqueous polyacrylamide solutions is pseudoplastic[44], i.e., the apparent viscosity decreases with increasing shear rate at relatively low shear rates.

A literature search showed that while a lot of information was found on the behaviour of polyacrylamide as a flocculant and coagulant in weak acid and alkaline conditions, less information was found on the behaviour of polyacrylamide in strong acid solutions such as copper electrolytes in 1.5-1.8M sulfuric acid.

Macromolecules such as high-molecular weight polyacrylamide such as 15 million Dalton Ciba Magnafloc® 800HP with theoretical lengths 10-50 μm, are used as flocculants and thickeners. Low-molecular-weight (co)polymers are used as coagulants and mud stabilizers due to their exceptional adsorption properties[48, 49]. Polyacrylamide adsorption onto solid surfaces may involve one or more of a number of interactions, listed below:

(i) Chemical short distance interactions, i.e., covalent bonding, coordination bonding, and hydrogen bonding;

(ii) Physical longer-range forces, i.e., electrostatic bonding, dipole attraction, London-van der Waals attraction;

(iii) Hydrophobic associations, i.e., surface hydrophobicity and substitutional adsorption with water, and endothermic adsorption process; and

(iv) Chemical nature of the surface, the presence of solutes and functional groups in the polymer[48].

Neutral or nonionic polyacrylamide, shown in Figure 2-5, confers adsorption through hydrogen bonding from the acrylamide functional group ($-CONH_2$). *Hydrolysed polyacrylamide,* shown in Figure 2-6, is frequently referred to as anionic polyacrylamide and consists of acrylamide-acrylic acid copolymers.

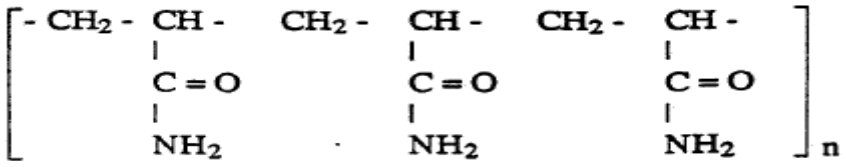

Figure 2-5: Nonionic polyacrylamide

It should be noted that while under neutral conditions nonionic polyacrylamide is stable; but under acidic or basic conditions it undergoes hydrolysis. The hydrolysis mechanisms are discussed in the next Sections.

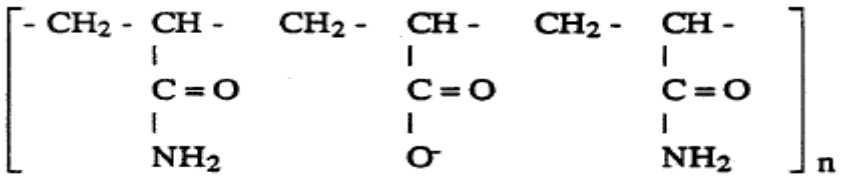

Figure 2-6: Anionic or hydrolysed polyacrylamide

2.6.2 Polyacrylamide Hydrolysis Mechanisms

Polyacrylamide undergoes hydrolysis in alkaline and acid solutions and the reaction product differs[50]. It is also known that that the kinetics of polyacrylamide hydrolysis depends on temperature, media and degree of shear. Hydrolysis of non-ionic polyacrylamide (described below) is the transformation of the amide functional group ($CONH_2$) of the polyacrylamide molecules to produce carboxyl functional group ($COO–$) and ammonia[51]. The percent of hydrolysis, τ is be defined as the number of carboxyl groups replacing amide groups divided by the total number of macromolecule groups, $\tau = 100y/(x + y)$ as described below:

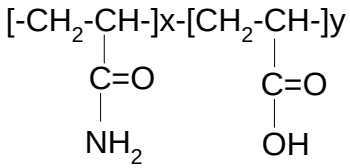

The number of negative charges on the polymer chain increases as a result of the polymer hydrolysis. This depends on the pH.

2.6.2.1 Polyacrylamide Hydrolysis in Neutral and Alkaline Solutions

Hydrolysis in water at room temperature is negligible (<2 percent)[52]. Polyacrylamide hydrolysis under basic reaction conditions at 60-100°C involves a nucleophilic addition of hydroxide to the amide carbonyl followed by the elimination of the amide ion ($-NH_2$) to afford an acrylic acid residue[50]. The amide ion then removes a proton from the acrylic acid residue to form a more stable carboxylate anion and ammonia as it is shown in the reaction pathway 1 below.

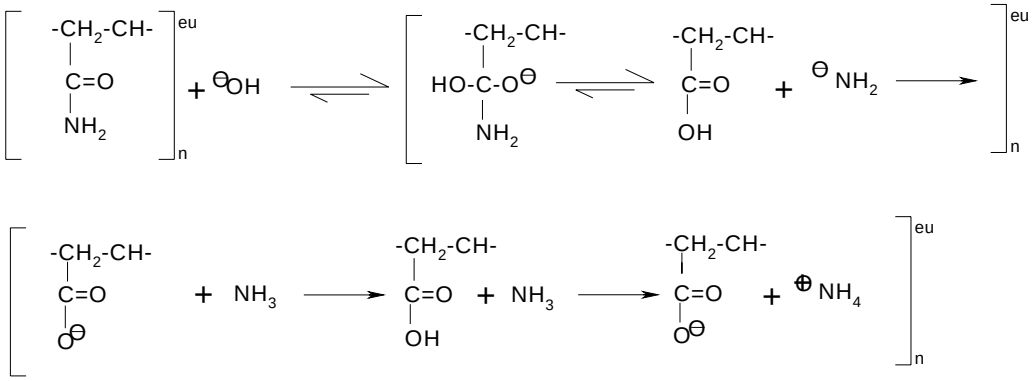

eu (either/unknown): polymer repeat pattern

Reaction Path 2.1: Hydrolysis of Polyacrylamide Under Alkaline Conditions[50]

Atkins[53] patented the hydrolysis of polyacrylamide to produce polyacrylic acid in sodium hydroxide at 50°C and reported a conversion of 30 and 61% after two and three hours residence time, respectively. Caulfield[50] reported that hydrolysis becomes extremely slow when the residual amide content falls below about 30% in the polyacrylamide.

2.6.2.2 Polyacrylamide Hydrolysis in Acid Solutions

Under acid conditions, polyacrylamide hydrolysis involves the nucleophilic addition of water to the protonated amide followed by the loss of ammonia as shown in the reaction pathway 2 below[50].

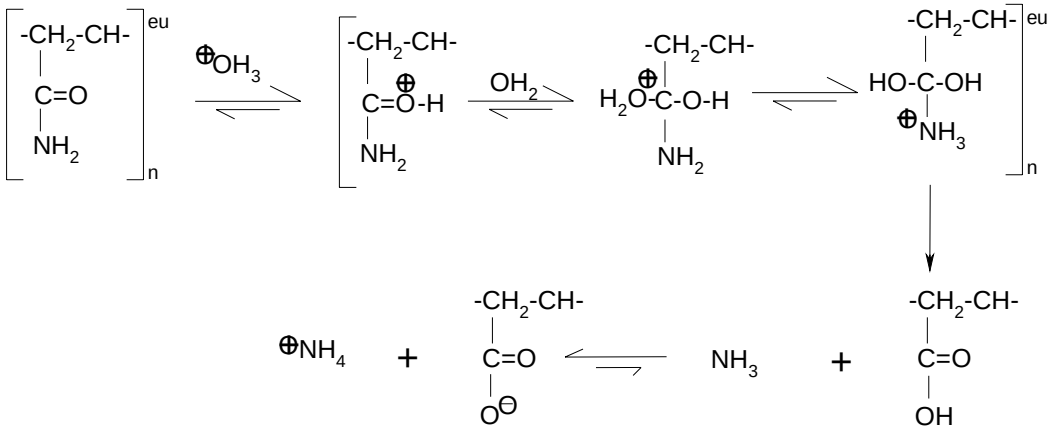

Reaction Path 2.2: Hydrolysis of Polyacrylamide under Acidic Conditions

Hydrolysis of polyacrylamide in strong acid solution can also lead to the formation of polyacrylimide (imide)[54, 55] shown in Figure 2-7. The *imide* is an insoluble gel induced in polyacrylamide either thermally or by mineral acids[56, 57].

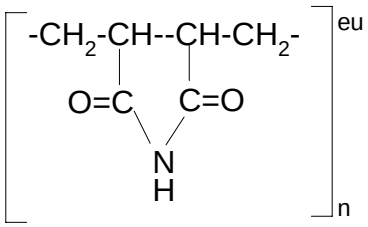

Figure 2-7: Polyacrylimide Molecule

The rapid initial reaction was characterised by the transient appearance of an absorption band at 235nm which was attributed to the formation of cyclic imide intermediate[50]. The imide quickly decomposed to form the acrylic acid residue. The proposed reaction pathway for the initial hydrolysis of polyacrylamide is presented below[50].

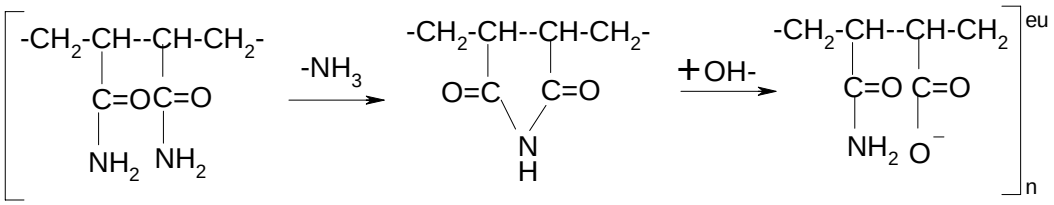

Reaction Path 2.3: Proposed Reaction Pathway for the Initial and Fast Hydrolysis of Polyacrylamide[50]

Minsk et al.[55] presented results for acid hydrolysis in the temperature range from below zero, 15, 38.5, 53.5, 65 and 73°C and for up to 22-hours. The *imide* content increased from 8.5 to 34.5% and the acrylic acid from 1.57% to 11.10%.

Moradi-Araghi et al.[54] presented similar data at 90°C, as summarised in Table 2-2. It can be seen that the per cent population of *imide* in concentrated acid increased steadily over 9 days and the carboxylate structure increases in a dilute base but the amide is the predominant functional group at any pH. In weakly acid solutions both authors reported very low concentrations of carboxylic acid and imide.

Table 2-2: Effect of Hydrolysis Media on the Population of Various Structures Starting from Non-hydrolysed Polyacrylamide[54]

Media	Ageing Time	Population, %		
	Days	Amide	Carboxylate	Imide
Dilute Base	0	84.5	14.2	1.3
Dilute Base	3	73.1	25.3	1.6
Dilute Base	0	84.5	14.2	1.3
Dilute Base	3	73.1	25.3	1.6
Dilute Acid	0	95.2	0.6	4.2
Dilute Acid	3	89	3	8.1
Dilute Acid	0	91.9	5	3.1
Concentrated Acid	0	94.4	0.8	4.7
Concentrated Acid	2	79	2.4	18.6
Concentrated Acid	9	71.7	2.5	25.8

Halverson et al[56] investigated the structural changes of polyacrylamide macromolecule from acid and alkaline hydrolysis using ^{13}C NMR and derived a sequence length of carboxyl groups in the polyacrylamide chain. These authors described structural characteristics within the polymer chain, with the implicit understanding that many chains are present, using the notation 'A' for the acrylamide functional group in the polymer and 'B' for the acrylic acid functional group (whether

in acid or base form). Additionally, the mole fraction of A units having only A units as nearest neighbours are denoted by F(AAA), the mole fraction of A units having one A unit and one B unit as nearest neighbours by F(AAB) or F(BAA) and so forth were named.

Table 2-3 shows the structural difference between alkaline and acid hydrolysis of polyacrylamide at 110^{o}C after 24-hours[56, 58]. It can be seen that 57 per cent hydrolysis at pH 2 predominantly produced blocks of continuous acrylic acid or acrylamide segments, i.e., AAA and BBB functional groups but alkaline hydrolysis contains ABB, BAB, ABA triads. The B segments (acrylic acid functional group) from alkaline hydrolysis are well distributed along the chain with an average sequence length of 1.4. This average sequence length of carboxyl groups from pH 2 acid hydrolysis was 14[58]. Moreover, the blocky polymers obtained at pH 2 acid hydrolysis appear to exhibit adsorption by covalent bonding or "salt linkage" where electrons are transferred from the acrylate group to multivalent cations like calcium and iron present in or on the mineral surface[56, 58]. The presence of polyacrylimide was also insignificant under both conditions of hydrolysis.

Table 2-3: Hydrolysis Level and Triad Mole Fractions[56, 58]

Media	Hydrolysis,%	AAA	AAB	BAB	ABA	ABB	BBB	Imide
Mild Alkaline	56	0.00	0.10	0.32	0.22	0.36	<0.01	---
Acid pH 2	57	0.31	0.07	0.00	0.00	0.08	0.49	0.04

As the pH 2 acid hydrolysis time for Table 2-3 was 24 hrs, it would be expected that the conversion of F(AAA) to F(BBB) in few hours of hydrolysis would be less complete, i.e., F(AAA) higher than 31%.

In slightly acidic solutions the rate of polyacrylamide hydrolysis increased with increasing temperature and decreasing pH and indicated conformation or structural changes of the polymer in solution upon degradation[59]. Light scattering data also under slightly acidic condition, suggested that the molecular weight of the polymer remained relatively "static" during the hydrolysis[59].

2.6.3 Polyacrylamide Adsorption Mechanisms

This section examines the adsorption of polyacrylamide predominantly onto either oxide or quartz surfaces in mildly acidic or alkaline conditions or onto gold and mild steel surfaces in strong acid solutions.

Neutral or nonionic polyacrylamide (PAM) confers adsorption through hydrogen bonding from the acrylamide functional group as shown in Figure 2-8[48, 60]. This was confirmed using the Scheutjens-Fleer adsorption isotherm in which the participation of segments as trains, loops and tails were calculated[18]. Increasing of the MW of PAM increases adsorption on hematite but its adsorption decreases from pH 3 to 9[61].

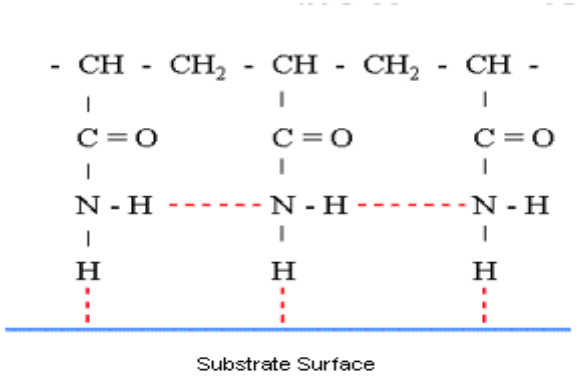

Figure 2-8: Hydrogen Bonding of Non-ionic Polyacrylamide

The presence of positively charged, negatively charged, and neutral chain segments in hydrolysed PAM confers amphoteric character on the polymer chain. The specific amphoteric interaction, typical of nonionic polyacrylamide, progressively disappears as the hydrolysis conversion increases until the non-selective interfacial surface coverage of polyacrylic acid takes place[48]. Therefore, the *number and distribution of –COOH groups* in polyacrylamide macromolecules determines the polymer chain conformation at the interface and directly influences the adsorption amount of polyacrylamide[48, 49, 51, 61]. Adsorption of polyacrylamide with few –COOH groups onto negatively charged surfaces is reduced due to the electrostatic repulsion between negatively charged carboxyl groups of the polymer and negative surface sites[49].

Polyacrylamide with blocks of carboxyl groups spaced along the polymer chain exhibit some adsorption properties which are different from their counter parts with carboxyl groups more widely distributed along the polymer chain particularly in the presence of divalent ions[58, 62]. This type of adsorption is shown in Figure 2-9. Moreover, adsorption takes place only if the energy of a segment-surface interaction is lower than that of a solvent-surface interaction, given by the adsorption energy, and is proportional to the number of adsorbed segments[63].

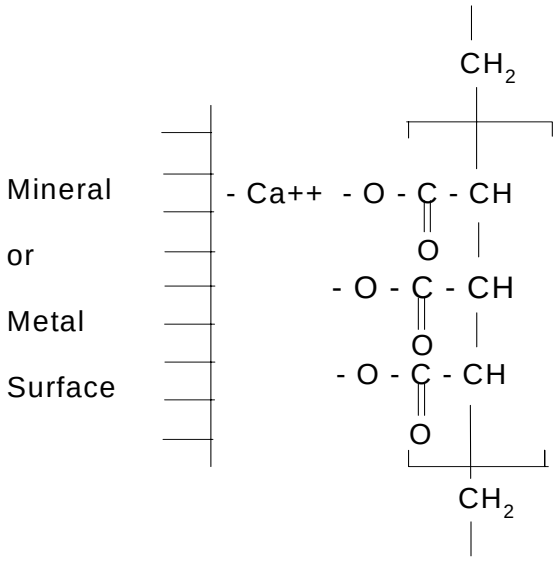

Figure 2-9: Blocky polyacrylamide may exhibit covalent bonding with divalent ions Calcium and Iron [64]

2.6.3.1 Polyacrylamide Adsorption onto Metals and Metal Alloy

It appears from the literature that only Grchev et al.[64-66] studied nonionic polyacrylamide adsorption in strong acid solutions. These authors indicated that adsorption of polyacrylamide on *gold* and *mild steel* in 0.5M sulfuric acidic solution strongly depends on the molecular weight of the polymer, electrode potential and temperature and it appears to be better described by the Frumkin isotherm than by the Langmuir isotherm[64-66]. The following conclusions were drawn from these studies:

(i) Polyacrylamide with a molecular weight of $5x10^3$ (g/mol) produced a surface coverage on gold close to 1 at 20°C and decreased to 0.25 surface coverage at 80°C. Adsorption at E=0 V (vs. MSE) and 40°C of 20 mg/L of $5x10^5$ Daltons

polyacrylamide yielded coverage value of approximately 0.6 and with $1.5x10^6$ molecular weight yielded 0.5. Similar values were obtained for mild steel in 1.6M HCl.

(ii) The value of the maximum coverage at about 20mg/L polyacrylamide and in the temperature range from 20 to 80^oC remains almost unaffected by the polymer molecular weight. Therefore, it is possible that the thickness of the adsorbed layer is not influenced by the polymer molecular weight and probably a flat orientation of the adsorbed parts of the polymer molecules on the metal surface takes place.

(iii) The surface coverage at 2-3mg/L polyacrylamide concentration decreased from about 0.52 to 0.02 as the polyacrylamide molecular weight increased from $5x10^3$ to $1.5x10^6$, respectively.

(iv) The effects of the adsorption of polyacrylamide on gold and mild steel were explained in terms of substitutional absorption of the polymer on a bare metal surface followed by a significant de-sorption of water molecules from the surface[51, 64-66]. The inhibition (adsorption) efficiency drastically decreased after 5-10 hours.

AFM studies of polyacrylamide adsorption on mica have been reported[67, 68]. Nonionic Polyacrylamide with 5.71 x 10^5 Dalton MW was synthesised to have $–SCH_2COOH$ as one end and $–CH_3$ as the other end confers covalent bonding with gold surfaces via the gold-sulfur bond and the rest of the macromolecules confers hydrogen bonding with mica in water. As the force-distance measurements between gold and sulfur were one order of magnitude greater than that between hydrogen bonding with mica and gold, the gold-sulfur bond was called *specific adsorption* and the hydrogen bonding as *non-specific adsorption*.

Polyacrylamide with 1500 and 10,000 Dalton MW at 100ppm concentration and pH 3 gave 1.22 and 1.84nm, respectively of adsorption layer thickness on hematite and the number of segments remained almost unchanged from about 2 to 10^{61}. Polyacrylic acid (PAA) with 2000 and 240,000 MW also at 100ppm concentration and pH 3 gave

1.73 and 2.65nm of adsorption layer thickness and an increase in the number of segments from 3 to 141[61], respectively. Chibowski et al.[61] therefore concluded that the length of both loops and tails may influence the adsorption layer thickness of PAM on hematite surfaces[61] and in contrast mainly tails of PAA are responsible for the increase of adsorption layer with the increase of MW.

2.6.3.3 Cleavage of Polyacrylamide

Polyacrylamide degradation defined as cleavage of the backbone chain can be initiated by different radicals, e.g., sulfate ions $SO_4^{=}$ or OH radicals obtained from decomposition of potassium and ammonium persulfate, H_2O_2-$FeSO_4$ in water, and temperature[69]. These radicals *abstract* an H atom from the "weak" units of the chain, primarily from the head-to-head structure polymer chain, which at low polymer concentration results in cleavage of C-C bond in the backbone. Oxygen also affects the stability of polyacrylamide solutions, i.e., oxidative degradation of polyacrylamide also occurs in the presence of oxygen[69]. Since copper EW electrolyte contains oxygen at its saturated concentration due to the dissociation of water, it may also contribute to the cleavage of PAM.

2.6.3.4 Adsorption Mechanism of Polyacrylamide

A general example of polyacrylamide adsorption has been reported as it is shown in Figure 2-10[63]. It proposes that in order to minimise the adsorption energy the adsorbed layer consists of polymer chains (amide group functionalities) with several stretches of segments in the surface layer (trains). Some trains stick out into the solution (loops rich in carboxylic acid functional groups). Moreover, at the chain ends, freely dangling tails may protrude into the solution.

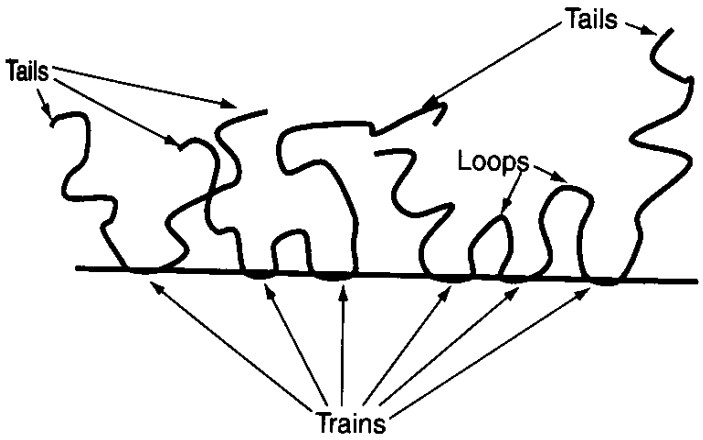

Figure 2-10: Postulated Structure of Adsorbed Partially Hydrolysed Polyacrylamide Layer at the Copper-Electrolyte Interface

However, this example needs to be re-examined to account for the charge density of a block copolymer and random polymer, and of the substrate. It was stated by Panzer and Halverson[58, 62] that polyacrylamide with blocks of carboxylic groups spaced along the polymer chain exhibit different adsorption properties, i.e., covalent bonding, particularly in the presence of divalent ions than random copolymers. Moreover, nonionic polyacrylamide, synthesized with sulfur at one tail to give $-SCH_2COOH$, exhibited covalent bonding or specific adsorption between the sulfur and a gold-plated cantilever during atomic force microscopy (AFM) studies[68].

There appears to be no published work studying the adsorption of block or random copolymers derived from polyacrylamide on copper metal. It would be enormously useful if research would be undertaken to determine if the findings of Halverson et al.[56] and Panzer and Halverson[58] could be extended to the adsorption of block and random polymers on copper. It is important to describe the adsorption mechanism to understand the observation that Mt. Gordon occasionally produced unusually smooth copper cathode when polyacrylamide was contacted with the pregnant leach solution at a pH value of about 1.5.

2.7 Summary

The aim of this chapter is to primarily highlight the importance of the addition of additives in copper electrodeposition. The nucleation and growth of copper electrodeposits needs to be controlled by the addition of carefully selected and properly concentrated organic additives to eliminate the formation of dendrites. In summary, the mechanism and electrochemical action of Guar and chloride ions have been poorly documented in the literature compared with those of glue, thiourea and chloride ions for electrorefining operations. Studies of the effect of polyacrylamides on copper electrodeposition are lacking. Therefore, a better understanding of the influence of polyacrylamide and Guar on copper electrocrystallization is particularly important. Chloride ions depolarize the electrode, in other terms increases the rate kinetics of the electrode-transfer and consequently increases surface roughness since it enhances growth rate rather than nucleation rate[32].

It is shown in Table 1-1 that only *two* additives are used in copper electrowinning: Guar, known in the industry as a "weak levelling agent" and chloride ions instead of *three* additives in copper electrorefining and *four* additives in the microelectronics industry. It may be due to the belief that the highly purified electrolyte solution obtained after solvent extraction does not require a levelling agent and the concern that a new organic additive may affect the solvent extraction reagent. However, it is known that in the damascene process[70] reagent grade electrolyte is used, but nevertheless a levelling agent, grain refiner and chloride ions are also dosed. Since the damascene process uses three additives (inhibitor, accelerator and chloride ions) rather than the two additives in conventional electrowinning it is concluded that electrowinning may be improved through the use of a levelling agent and grain refiner besides chloride ions to control dendrite growth and minimize the level of impurities in the copper cathode. At the commencement of the work described in this thesis, it was not known whether polyacrylamide behaved as a levelling agent or grain refiner or both.

Vereecken and Winand[41] concluded that the quality of the copper deposits obtained with Guar was always better than those obtained with both nonionic and cationic polyacrylamides. Vereecken and Winand[41] also observed the depolarization

behaviour of nonionic and cationic polyacrylamides, and Guar prepared in water or in a solution of pH 3.

The physicochemical properties of polyacrylamide can be summarized as follow:

(i) Polyacrylamide adsorption onto solid surfaces may involve both chemical and physical adsorption. The adsorption of polymers also depends on the solution pH, chemical nature of the surface, the presence of solutes and the functional groups of the polymer.

(ii) The reaction pathway and therefore product from alkaline hydrolysis is different to that from acid hydrolysis. Polyacrylamide in a strong acid medium is attached to the surface through hydrogen bonds. Hydrolysis increases the number of carboxyl functional groups in the polymer.

(iii) The reaction product of non-ionic polyacrylamide hydrolysed in strong acid conditions is polyacrylimide upon ageing. However, the presence of polyacrylimide was insignificant under slightly acidic conditions.

(iv) Light scattering data indicates that under slightly acidic condition the molecular weight of the polymer remained relatively "static" during the hydrolysis process.

(v) Hydrolysis at pH value of 2 predominantly produces blocks of acrylic acid and acrylamide segments with an average sequence length of carboxyl groups of 14 instead of 1.4 obtained from alkaline hydrolysis.

(vi) In general, the *initial hydrolysis* of polyacrylamide is faster than the remainder[50].

(vii) Literature on the adsorption of PAM on copper metal and 316L stainless steel appears to be nonexistent. However, the free energy of the overall adsorption process of the polyacrylamide pre-treated at pH value of 1.5 must be favourable if it is going to be a useful organic additive in copper electrowinning and electrorefining.

(viii) The adsorption process of non-ionic and anionic PAM and also polyacrylic acid depends on their molecular weight (MW), solution pH, hydrophobicity characteristics of the substrate[71] and the presence of some metal chlorides[61].

2.8 References

1. Robinson T, Davenport WG, Quinn J, Karkas G. Electrolytic Copper Refining - 2003 World Tankhouse Operating Data. In: Dutrizac JE, Clement CG, editors. *Copper 2003 - Cobre 2003*; 2003; Santiago, Chile: Canadian Institute of Mining, Metallurgy and Petroleum; 2003. p. 3-66.

2. Robinson T, Rasmussen S, Davenport WG, Jenkings J, King M. Copper Electrowinning - 2003 World Tankhouse Operating Data. In: Dutrizac JE, Clement CG, editors. *Copper 2003 - Cobre 2003 Copper Electrorefining and Electrowinning*; 2003; Santiago, Chile; 2003. p. 421-472.

3. Baxter K, Kaiser C, Richmond GD. Design of the Mt. Gordon Chalcocite Project. In: *Alta Copper Sulfides Symposium*; 1999 September 5-10; 1999. p. 1-21.

4. Richmond G, Christie M. The Commissioning and Operation of a Copper Sulfide Pressure Oxidation Leach Process at Mt. Gordon. In: ALTA, editor. *Alta Copper Sulfides Symposium*; 1999 September 5-10; 1999. p. 1-9.

5. Richmond G, Dreisinger D; inventors. Western Metals Copper Limited, assignee. Processing Copper Sulfide Ores. Australia patent 749257. 1999.

6. Vetter K. *Electrochemical Kinetics, Theoretical and Experimental Aspects*. New York: Academic Press; 1967.

7. Budevski E, Staikov G, Lorenz W. *Electrochemical Phase Formation and Growth, an Introduction to the Initial Stages of Metal Deposition*. New York: VCH; 1996.

8. Paunovic M, Schlesinger M. *Fundamentals of Electrochemical Deposition*: John Wiley & Sons, Inc.; 1998.

9. Bard AJ, Faulkner L. *Electrochemical Methods, Fundamentals and Applications*. Second ed. Brisbane: John Wiley & Sons, Inc.; 2001.

10. Newman J, Thomas-Alyea KE. *Electrochemical Systems*. Third ed. Hoboken, New Jersey: John Wiley & Sons, Inc.; 2004.

11. Grabowski A, Newman J. *Current and Potential Distributions on a Cylinder Electrode*. J. Electrochem. Soc. 1993;140(6):1625-1631.

12. Gabe D. *Rotating Electrodes for Use in Electrodeposition Process Control*. Plating & Surface Finishing 1995;9:69-76.

13. Podlaha E, Landolt D. *Induced Codeposition Ii. A Mathematical Model Describing the Electrodeposition of Ni-Mo Alloys*. J. Electrochem. Soc. 1996;143(3):893-899.

14. Eisenberg M, Tobias C, Wilke C. *Ionic Mass Transfer and Concentration Polarization at Rotating Electrodes*. Journal of the Electrochemical Society 1954;101(6):306-319.

15. Arvia AJ, Carrozza JSW. *Mass Transfer in the Electrolysis of Cuso4-H2so4 in Aqueous Solutions under Limiting Current and Forced Convection Employing a Cylindrical Cell with Rotating Electrodes*. Electrochimica Acta 1962;7:65-78.

16. Barkey D, Muller R, Tobias C. *Roughness Development in Metal Electrodeposition I. Experimental Results*. Journal of the Electrochemical Society 1989;138(8):2199-2207.

17. Gabe D, Wilcox G, Gonzalez-Garcia J, Walsh F. *The Rotating Cylinder Electrode: Its Continued Development and Application*. Journal of Applied Electrochemistry 1998;28(8):759-780.

18. Maciel J, Agostinho S. *Construction and Characterization of a Rotating Cylinder Electrode for Different Technological Applications*. Journal of Applied Electrochemistry 1999 Jun;29(6):741-745.

19. Filzwieser A, Hein K, Hanko G. Application of Two Phase Hydrodynamic Modeling to an Electrowinning Cell. In: Dutrizac JE, Ji J, Ramachandran V, editors. *Copper 99 - Cobre 99 International Conference*; 1999: The Minerals, Metals & Materials Society; 1999.

20. Manzanares JA, Kontturi K. Diffusion and Migration. In: Calvo EJ, editor. *Interfacial Kinetics and Mass Transport*: Wiley-VCH; 2003. p. 81-121.

21. Wang L, Olsen M, Vigil R. *Reappearance of Azimuthal Waves in Turbulent Taylor-Couette Flow at Large Aspect Ratio*. Chemical Engineering Science 2005;60:5555-5568.

22. Schlichting H. *Boundary-Layer Theory*. Sydney: McGraw-Hill; 1968.

23. Silverman DC. *The Rotating Cylinder Electrode for Examining Velocity-Sensitive Corrosion - a Review*. Corrosion 2004;60(11):1003-1022.

24. Newman J. *Electrochemical Systems*. Second ed. London: Prentice-Hall International; 1991.

25. Bard AJ, Parsons R, Jordan J. *Standard Potentials in Aqueous Solution*. New York: Marcel Dekker, Inc; 1985.

26. Mattsson E, Bockris JOM. *Galvanostatic Studies of the Kinetics of Deposition and Dissolution in the Copper+Copper Sulphate System*. Transaction Faraday Soc. 1959;55:1586-1601.

27. Calvo EJ. The Current-Potential Relationship. In: Bard AJ, Stratmann M, editors. *Encyclopedia of Electrochemistry, Volume 2: Interfacial Kinetics and Mass Transport*: Wiley-VCH; 2003. p. 3-30.

28. Dini J. *Electrodeposition, the Materials Science of Coatings and Substrates*. New Jersey: Noyes Publications; 1993.

29. Sun M, O'Keefe T. *The Effect of Additives on the Nucleation and Growth onto Stainless Steel Cathodes*. Metallurgical Transaction B 1992;23B:591-599.

30. Zhou Z, Okeefe T. *Electrodeposition of Copper on Thermally Oxidized 316 L Stainless Steel Substrates*. Journal of Applied Electrochemistry 1998(4):461-469.

31. Kinaci F. Nucleation and Growth in Electrodeposition of Thin Copper Films on Pyrolytic Graphite [MS]. Berkeley: University of California; 1992.

32. Ilgar E, O'Keefe T. Surface Roughening of Electrowon Copper in the Presence of Chloride Ions. In: Dreisinger D, editor. *Aqueous Electrotechnologies: Progress in Theory and Practice*; 1997: The Minerals Metals and Materials Society; 1997. p. 51-62.

33. Wu Q, Barkey D. *Faceting and Roughening Transitions on Copper Single Crystals in Acid Sulfate Plating Baths with Chloride*. Journal of the Electrochemical Society 2000 Mar;147(3):1038-1045.

34. Chassaing E, Wiart R. *Epitaxial Growth and Electrode Impedance of Copper Electrodeposits*. Electrochimica Acta 1984;29(5):649-660.

35. Gabrielli C, Mocoteguy P, Perrot H, Wiart R. *Mechanism of Copper Deposition in a Sulfate Bath Containing Chlorides*. Journal of Electroanalytical Chemistry 2004;572(2):367-375.

36. Radisic A, West A, Searson P. *Influence of Additives on Nucleation and Growth of Copper on N-Si(111) from Acidic Sulfate Solutions*. Journal of the Electrochemical Society 2002;149(2):C94-C99.

37. Schmidt W, Alkire R, Gewirth A. *Mechanic Study of Copper Deposition onto Gold Surfaces by Scaling and Spectral Analysis of in-Situ Atomic Force Microscopic Images*. J. Electrochem. Soc. 1996(10):3122-3132.

38. Kang M, Gross ME, Gewirth AA. *Atomic Force Microscopy Examination of Cu Electrodeposition in Trenches*. Journal of the Electrochemical Society 2003;150(5):C292-C301.

39. Hope GA, Woods R. *Transient Adsorption of Sulfate Ions During Copper Electrodeposition*. J. Electrochem. Soc. 2004;151(9):C550-553.

40. Pye D, Schurz G; inventors. The Dow Chemical Company, assignee. Electrowinning of Metals. United States patent 2,798,040. 1957 July 2, 1957.

41. Vereecken J, Winand R. *Influence of Polyacrylamides on the Quality of Copper Deposits from Acidic Copper Sulphate Solutions*. Surface Technology 1976; 4:227-235.

42. Langner BE, Stantke P, Reinking EF; inventors. Norddeutsche Affinerie Aktiengesellschaft (Hamburg, DE), assignee. Method of Measuring the Effective Inhibitor Concentration During a Deposition Process of Metal from Aqueous Electrolytes and Test Apparatus Therefore patent 4,834,842. 1989.

43. Stantke P. *Guar Concentration Measurement with the Collamat System*. Proceedings of the COPPER 99-COBRE 99 International Conference 1999;3:643-651.

44. Mark H, Gaylord N, Bikales N. *Encyclopedia of Polymer Science and Technology*; 1969.

45. Lipkowski J. *1998 Alcan Award Lecture - Surface Electrochemistry - Surface Science with a Joy Stick*. Canadian Journal of Chemistry 1999;77(7):1163-1176.

46. Saban M, Scott J, Cassidy R. *Collagen Proteins in Electrorefining: Rate Constants for Glue Hydrolysis and Effects of Molar Mass on Glue Activity*. Metallurgical & Materials Transactions B-Process Metallurgy & Materials Processing Science 1992;23B:125-133.

47. Plieth W. *Additives in the Electrocrystallization Process*. Electrochimica Acta 1992;37(12):2115-2121.

48. Pefferkorn E. *Polyacrylamide at Solid/Liquid Interfaces*. Journal of Colloid & Interface Science 1999;216:197-220.

49. Drzymala J, Fuerstenau D. *Adsorption of Polyacrylamide, Partially Hydrolyzed Polyacrylamide and Polyacrylic Acid on Ferric Oxide and Silica*. Process Technology Proceedings 1987;4(Flocculation Biotechnol. Sep. Syst.):45-60.

50. Caulfield MJ, Qiao GG, Solomon DH. *Some Aspects of the Properties and Degradation of Polyacrylamides*. Chemical Reviews 2002;102(9):3067-3083.

51. Ghannam M. *Wetting Behavior of Aqueous Solutions of Polyacrylamide over Polyethylene Substrate*. Journal of Chemical and Engineering Data 2002;47(2):274-277.

52. Tackett J; inventor. Marathon Oil Company, assignee. A Method for Inhibiting Hydrolysis of Polyacrylamide patent WO 92/07881. 1992.

53. Atkins M, Biggin I, Kidd D; inventors. BP Chemicals Limited, assignee. Hydrolysis of Polymers. United States patent 5,081,195. 1992 January 14, 1992.

54. Moradi-Araghi A, Hsieh E, Westerman I. *Role of Imidization in Thermal Hydrolysis of Polyacrylamides*. Water-Soluble Polym. Pet. Recovery, [Proc. Natl. Meet. ACS] 1988:271-8.

55. Minsk L, Kotlarchik C, Meyer G, Kenyon W. *Imidization During Polymerization of Acrylamide*. Journal of Polymer Science 1974;12:133-140.

56. Halverson F, Lancaster J, O'Connor M. *Sequence Distribution of Carboxyl Groups in Hydrolyzed Polyacrylamide*. Macromolecules 1985;18(6):1139-44.

57. Haas H, Macdonald R. *Imidization Reaction in Polyvinylamides*. Journal of Polymer Science 1971;9(A-1):3583-3593.

58. Panzer H, Halverson F. Blockiness in Hydrolyzed Polyacrylamide. In: Moudgil B, Scheiner B, editors. *Flocculation Dewatering, Proc. Eng. Found. Conf.*; 1988; Palm Coast Florida, USA; 1988. p. 239-49.

59. Muller G, Fenyo J, Selegny E. *High Molecular Weight Hydrolyzed Polyacrylamides. Iii. Effect of Temperature on Chemical Stability*. Journal of Applied Polymer Science 1980;25:627.

60. Kuz'kin SF, Nebera VP, Zolin SN. *Aspects of the Theory of Suspension Flocculation by Polyacrylamides*. Intern. Mineral Process. Congr., Tech. Papers, 7th, New York City, 1964 1965;1:347-57.

61. Chibowski S, Wisniewska M. *Study of Electrokinetic Properties and Structure of Adsorbed Layers of Polyacrylic Acid and Polyacrylamide at Ferric Oxide-Polymer Solution Interface*. Colloids and Surfaces A: Physicochemical and Engineering Aspects 2002;208(1-3):131-145.

62. Panzer H, Halverson F, Lancaster J. *Carboxyl Sequence Distribution in Hydrolyzed Polyacrylamide*. Polymeric Materials Science and Engineering 1984;51:268-71.

63. Holmberg K, editor. *Handbook of Applied Surface and Colloid Chemistry*: John Wiley & Sons, Ltd.; 2002.

64. Grchev T, Cvetkovska M. *Electrochemically Initiated (Co)Polymerization of Acrylamide and Acrylonitrile on a Steel Cathode - Electrochemical and Impedance Study*. Journal of Applied Electrochemistry 1989;19(3):434-42.

65. Grchev T, Cvetkovska M, Stafilov T, Schultze J. *Adsorption of Polyacrylamide on Gold and Iron from Acidic Aqueous Solutions*. Electrochimica Acta 1991;36(8):1315-1323.

66. Grchev T, Cvetkovska M, Schultze JW. *The Electrochemical Testing of Polyacrylic Acid and Its Derivatives as Inhibitors of Corrosion*. Corrosion Science 1991;32(1):103-12.

67. Haschke H, Miles MJ, Sheppard S. *Adsorption of Individual Polyacrylamide Molecules Studied by Atomic Force Microscopy*. Single Molecules 2002;3(2-3):171-172.

68. Haschke H, Miles MJ, Koutsos V. *Conformation of a Single Polyacrylamide Molecule Adsorbed onto a Mica Surface Studied with Atomic Force Microscopy*. Macromolecules 2004;37(10):3799-3803.

69. Kurenkov V, Hartan H, Lobanov F. *Degradation of Polyacrylamide and Its Derivatives in Aqueous Solutions*. Russian Journal of Applied Chemistry 2002;75(7):1039-1050.

70. Vereecken PM, Binstead RA, Deligianni H, Andricacos PC. *The Chemistry of Additives in Damascene Copper Plating*. IBM Journal of Research and Development 2005;49(1):3-19.

71. Broseta D, Medjahed F. *Effects of Substrate Hydrophobicity on Polyacrylamide Adsorption*. Journal of Colloid and Interface Science 1995;170(2):457-465.

CHAPTER 3

EFFECT OF PREPARATION MEDIA OF POLYACRYLAMIDE ON SURFACE ROUGHNESS

3.1 Introduction

As discussed in the previous Chapter it is generally accepted that the mechanisms of polyacrylamide hydrolysis and the reaction products in acid and alkaline media are different. This difference mainly corresponds, to the distribution of the polyacrylic acid moieties in the polyacrylamide molecular chain: block copolymers appears to be obtained in slightly acidic solutions, i.e., pH 2 and random copolymers in alkaline solutions. However, in strong acid solutions the amount of polyacrylimide becomes a significant product upon ageing.

In the work described in this Chapter, the equipment required to carry out bulk electrolysis, a rotating cylinder electrode, was built and its characteristics in terms of diffusion layer thickness and surface roughness of electrowon copper were compared with those published in the recent literature. A rotating cylinder electrode (RCE) was selected as the electrode for copper electrowinning trials because at low rotation speeds this *large* electrode configuration appears to achieve *turbulent* flow with vortices described in Appendix A, a uniform current distribution and therefore mass transfer[1, 2]. The RCE allows the hydrodynamics of a commercial scale copper electrowinning cell to

be approximated at low speeds of rotation. The RCE primarily imposes horizontal forced convection thus minimizing the effect of the vertical free convection due to changes in density at the electrode/electrolyte interface.

It has been described in Chapter 1 that Mt. Gordon occasionally produced the smoothest copper cathode ever known in the industry. Therefore, the aim in this Section was to indirectly explore the range of hydrolysis products of polyacrylamide to achieve the smoothest copper deposit surface. Thus, polyacrylamide was prepared in both acid solutions (including diluted solutions of the full-strength electrolyte) and alkaline solutions. The experiments were designed to evaluate the effect of polyacrylamide preparation media on the surface roughness of the copper deposit obtained from copper electrowinning.

3.2 Experimental

3.2.1 Design and Construction of Rotating Cylinder Electrode for Copper Electrowinning

A rotating cylinder electrode was designed and constructed at the Engineering Workshop of James Cook University similar in design to that described by Barkey, Muller and Tobias[3]. Figures 3-11 and 3-12 present the design of the top and bottom sections of the rotating cylinder electrode, respectively. The main feature of the rotating cylinder electrode design is that it resembles a typical commercial scale operation in terms of (i) the distance between the electrodes, 40mm, (ii) the use of the industry-standard cathode material (316L stainless steel) and (iii) the hydrodynamics of the electrolyte.

The rotating cylinder electrode (RCE) for this thesis, consisted of a 4.445 cm diameter 15 cm overall height 316L stainless steel rod (Sandvik). This electrode was bounded tightly with 3mm thickness PTFE sleeves to suppress edge effects and to leave a 2cm active height of stainless steel exposed. A dimensionally stable anode (DSA) sourced from Eltech Systems Corporation (USA) was used for the anode of the RCE. The RCE with the DSA concentrically arranged around it was located within a 5L Pyrex beaker. Eight PTFE baffles (200 x 20 x 5 mm) within the beaker maintained the DSA mesh at a distance of 40 mm from the RCE surface through a PVC lid. The RCE electrowinning cell rested in a thermostated water bath.

The active area of the RCE was 27.91cm^2 and the number of coulombs applied to each test varied from 12,000 to 36,000C. The rate of rotation of the RCE was controlled using a Movitrac controller and 0.37kW motor (RF27DT71D4) using a gear box sourced from SEW Eurodrive.

In the experiments described in this Chapter, the dependent variable was the surface roughness of the copper electrodeposit produced.

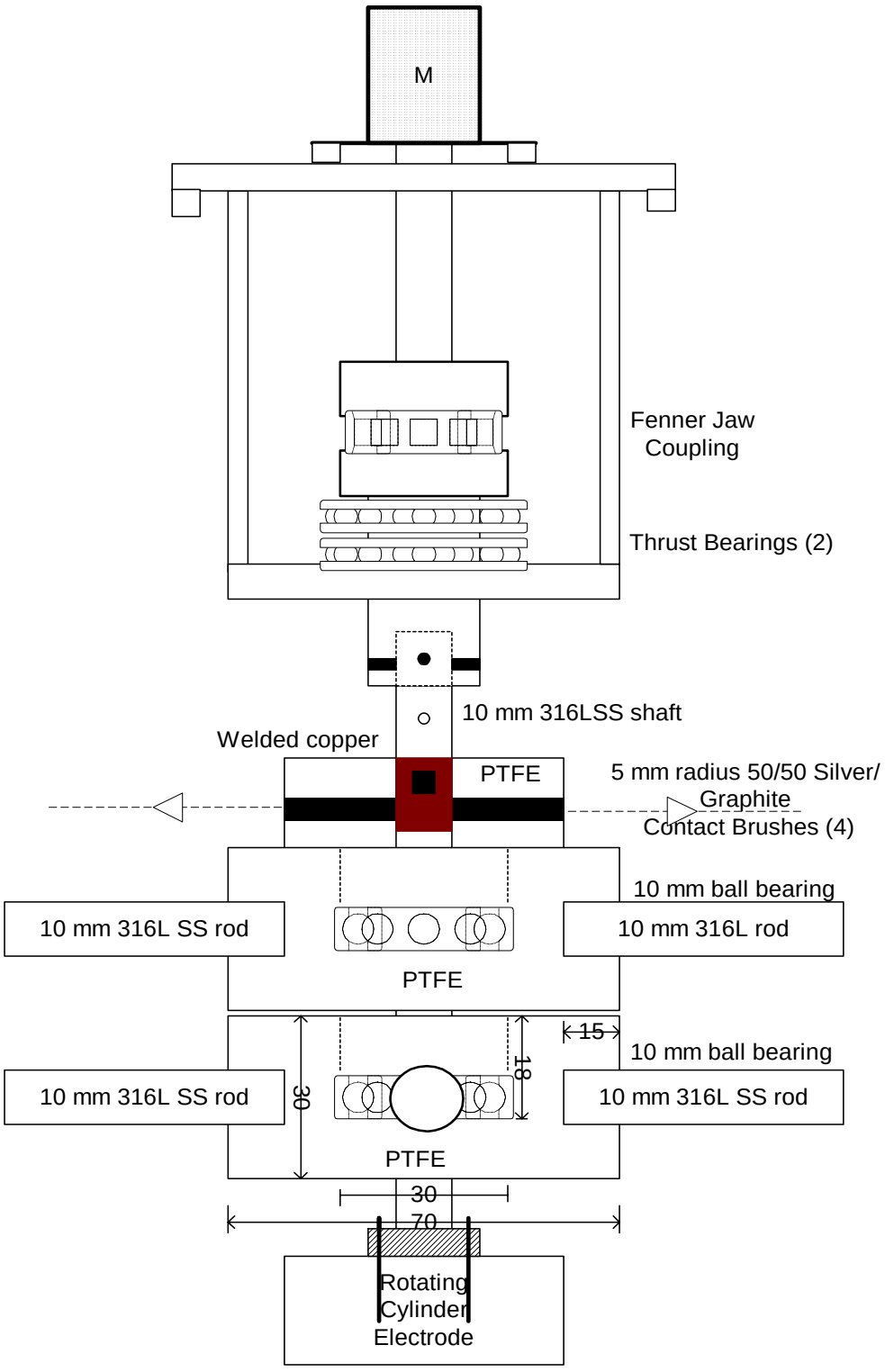

Figure 3-11: Rotating Cylinder Electrode – Top Section

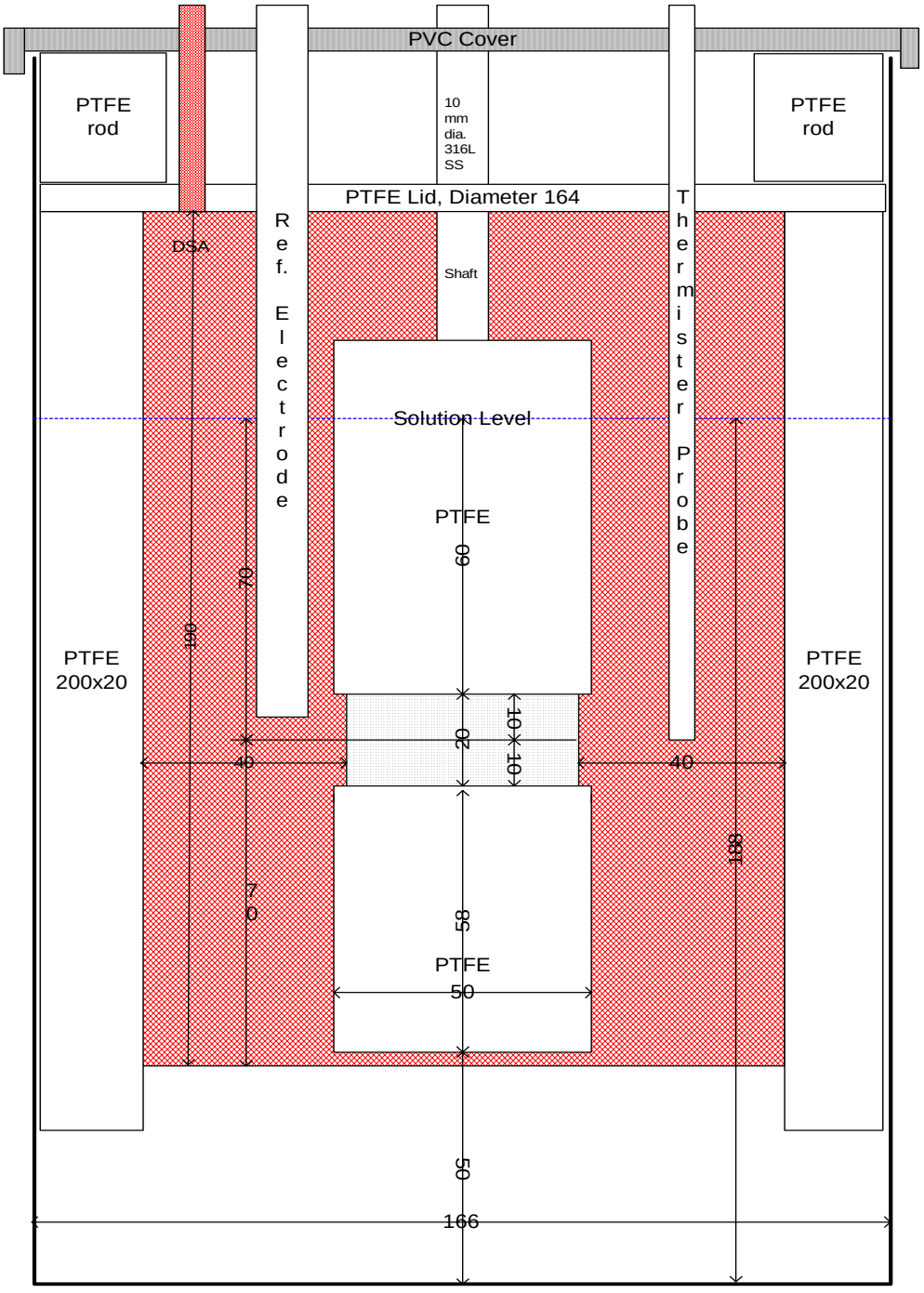

Figure 3-12: Rotating Cylinder Electrode – Bottom Section

The surface roughness was collected using a Mahr Perthometer M1[4] with a 2μm stylus tip radius. It was calibrated with its PGN-3 (Rz = 2.9μm, Ra = 0.79μm) standard. The surface roughness measurement was conducted before the copper deposit was detached from the rotating cylinder electrode along the height of the electrode. This measurement process was *repeated 8 times* around the cylinder electrode on equidistantly distributed lines. Figure 3-13 shows the setup of the rotating cylinder electrode and the M1 Mahr Perthometer to measure the surface roughness. Direct current to the RCE electrowinning cell was applied using a 0-18VDC, 0-20A digital power supply sourced from Cole-Parmer Extech Equipment Pty. Ltd., USA.

The copper deposit, a ring, was removed from the rotating cylinder electrode once the surface roughness measurements were obtained. The copper deposit ring was gently forced out using a stainless steel ring specially machined with an internal diameter of few microns larger than that of the RCE and a 2inch diameter stainless steel pipe (~20cm height). The stainless steel pipe was made to sit on the top of the stainless steel ring and hammered vertically using a mallet while the RCE sat on a 60mL plastic sampler (<4cm diameter). This procedure may occasionally produce few scratches onto the RCE but is does not affect the surface roughness measurement and it is a better technique than that used by Barkey et al. [3] who machined the RCE to have a slope of a few microns which could affect the current density distribution.

The RCE was polished with 1μm and 0.25μm diamond paste and had an initial surface roughness of 0.15 ± 0.04 μm. Once the copper was detached from the RCE, the RCE was immersed in 10% nitric acid for about 60 seconds, polished with 0.25μm diamond paste, washed with distilled water, immersed again in the nitric acid solution for another 60 seconds and completely washed with distilled water. This sequence was repeated after each test and the stainless steel maintained its brightness.

Figure 3-13: M1 Mahr Perthometer Measuring the Surface Roughness of Electrowon Copper

3.2.3 Determination of Limiting Current Density and Diffusion Layer Thickness

The aim in this section is to discuss the limiting current density, i_L technique to determine the diffusion layer thickness, δ for copper electrodeposition. The value of the diffusion layer thickness is then correlated with surface roughness in Section 3.2.4.

The δ was calculated in the literature either by measuring i_L for copper deposition[4-6] or by measuring the i_L for added silver[7, 8]. As silver is reduced at more positive potentials than copper by 0.462mV, it should plate at its mass transfer controlled (limiting) current density at the normal operating cathode potential (-100 to -300mV vs. Hg/H_2SO_4). The accuracy of both techniques may be limited by both the electrocrystallization mechanism on the particular substrate in terms of underpotential deposition and type of nucleation and growth[9-11]. It also is argued against the i_L technique applied directly to copper deposition that at current densities close to the i_L it gives powdery material increasing the active area of the working electrode and therefore

affecting the results[7]. In this thesis the i_L was measured using the copper electrodeposition method.

The large active area (27.91 cm^2) of the large rotating cylinder electrode used for all the testwork in this Chapter and Chapter 4 was an impediment to measure directly the i_L on that electrode due to the one ampere capacity of the instrumentation for this test. Therefore, i_L and δ were determined using a *small* RCE described and used in Chapter 5 – Figure 5-3. Appendix A shows that the i_L and δ are similar for both the large and small RCE. The electrolyte composition is described in Table 3-4. The first cycle of Cyclic Voltammograms at 1mV/sec with the RCE at 0, 10, and 25rpm and 45°C and 65°C in the absence of additives were used to determine the i_L. Figures 3-14, 3-15 and 3-16 show the results.

Table 3-4: Electrolyte Composition and Other Variables

Copper, g/L	36
Sulfuric acid, g/L	160
Chloride ions, mg/L	25
Active cathode surface area, cm^2	1.5
Electrolyte volume, mL	500
Inter-electrode distance, mm	32

The i_L for this thesis was also calculated using the equations developed by Eisenberg et al.[12] and Arvia et al[13], discussed in Section 2.3, and these equations are replicated as Equations 3-16 and 3-17, respectively. Although the equation of Eisenberg et al.[12] is valid for Reynolds numbers from 112 to 162,000 and Schmidt numbers from 2230 to 3650, it is known to be in error by as much as 8.3 percent[2].

$$i_L = 0.0791 \frac{nFDC_b}{di} (\mathrm{Re})^{0.7} (Sc)^{0.356} \qquad (3\text{-}16)$$

$$i_L = 0.0791\, nFC_b \left(\frac{di}{\nu}\right)^{-0.30} (U)^{0.70} \left(\frac{do}{di}\right) (Sc)^{-0.644} \qquad (3\text{-}17)$$

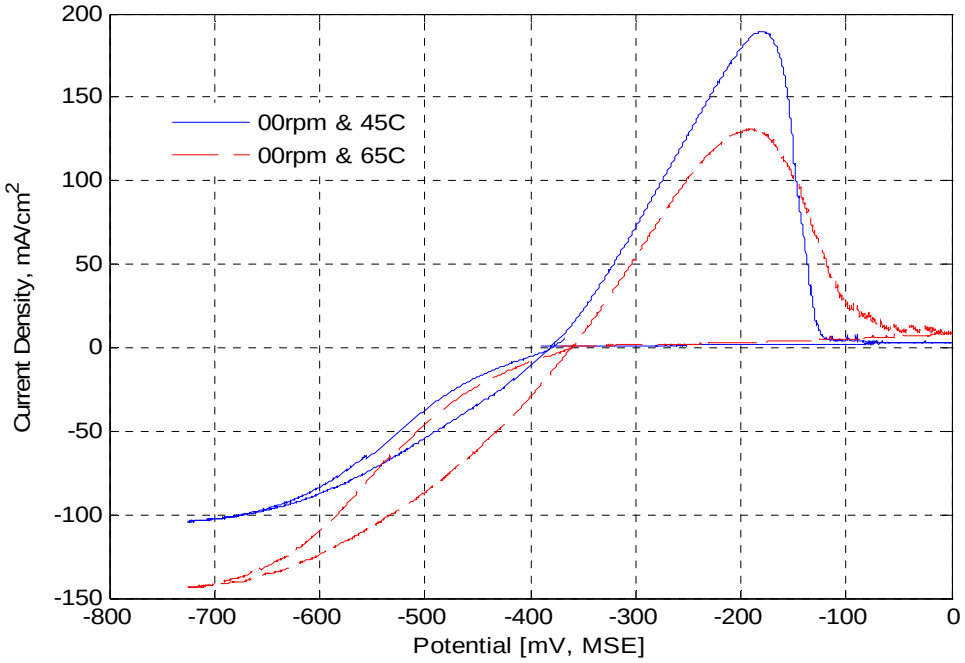

Figure 3-14: Current-Potential Curve – First Cycle Starting on pre-plated copper at 1mV/sec with the RCE at 0rpm (Free Convection) and 45°C and 65°C in the Absence of Additives to determine the Limiting Current Density (1037 and 1432 A/m^2).

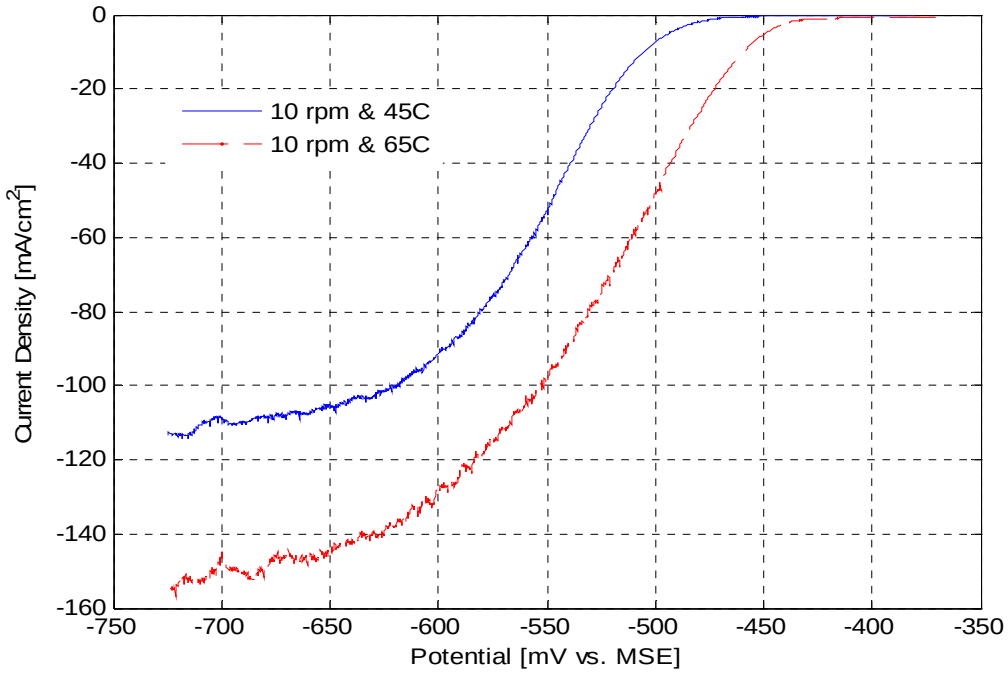

Figure 3-15: Current-Potential Curve – Initial Cycle Starting on Bare Stainless Steel at 1mV/sec with the RCE at 10rpm and 45 and 65°C in the Absence of Additives to determine the Limiting Current Density (1118 and 1497 A/m^2).

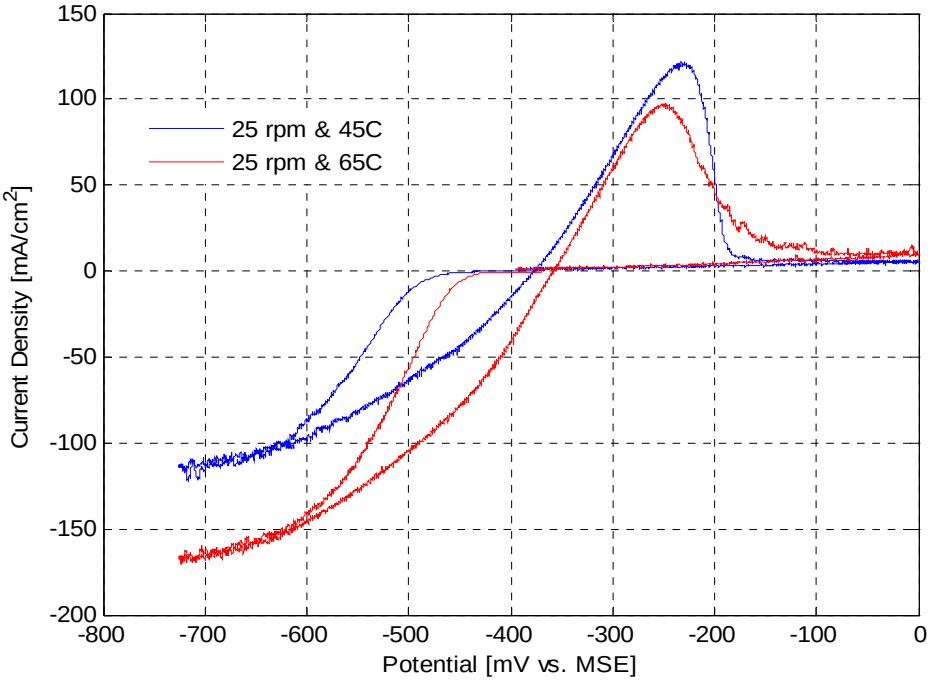

Figure 3-16: Current-Potential Curve – First Cycle Starting on Bare Stainless Steel at 1mV/sec with the RCE at 25rpm and 65°C in the Absence of Additives to determine the Limiting Current Density (1155 and 1666 A/m^2).

i_L is given by Fick's first law with a surface concentration of zero described in Equation 3-18[14].

$$i_L \equiv \frac{nFDC_b}{\delta} \tag{3-18}$$

where δ is the diffusion layer thickness. Recombination of equations (3-16) or (3-17) and (3-18) allows the diffusion layer thickness to be calculated. The δ is schematically shown in Figure 3-17. The concentration of cupric ions at the electrode/electrolyte interface is zero at the limiting current density.

It is shown in Appendix A that Arvia et al.'s[13] equation produces similar δ for both the large and small rotating cylinder electrodes used in this thesis and hence it is used to present the calculated value of δ.

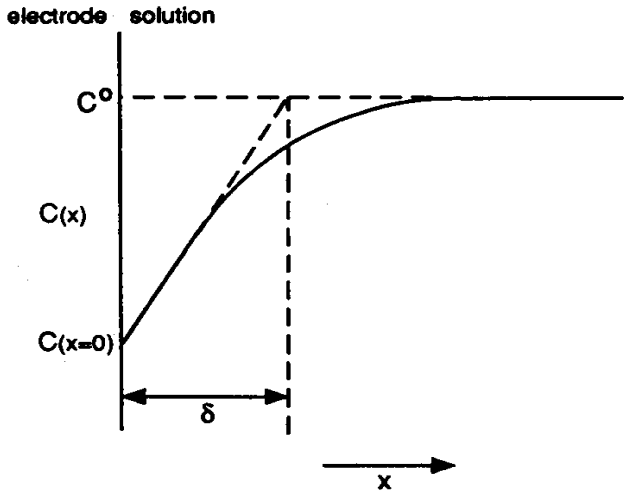

Figure 3-17: Schematic Presentation of the Concentration Profile of Cupric Ions (C^o at the bulk electrolyte) at the Electrode/ electrolyte Interface and the Diffusion Layer Thickness, δ.

In order to apply Equations 3-16 and 3-17 to calculate the diffusion layer thickness the kinematic viscosity and diffusion coefficient of cupric ions at different temperatures were required. The viscosity and electrolyte density for 35 g/L copper and 165 g/L sulfuric acid were obtained from Price et al.[15] to derive the kinematic viscosity at different temperatures as plotted in Figure 3-18. The diffusion coefficient of cupric ions was collected from various authors[1, 8, 16] for different temperatures and plotted in Figure 3-19. An exponential line of the best fit was used to fit the data and the diffusion coefficient at any temperature was determined by interpolation.

Appendix A presents the calculations to determine the diffusion layer thickness. Table 3-5 and Figure 3-20 present the summary of the results. The results obtained by using the equation developed by Arvia et al.[13] more closely replicate the experimental data than those obtained by using the equation developed by Eisenberg et al.[12]. These findings are consistent with an effect of sulfuric acid discussed in Section 2.3. Therefore diffusion layer thicknesses obtained using Arvia et al.'s[12] equation were compared with the data for this thesis as depicted in Figure 3-20.

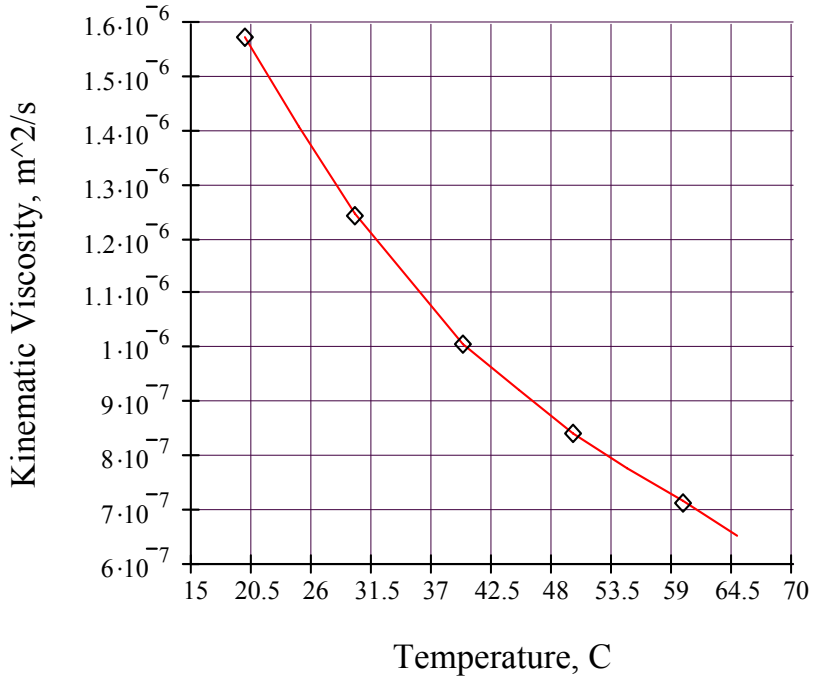

Figure 3-18: Variation in Kinematic Viscosity with Temperature

◊ represents Price et al.'s[15] data for a copper electrolyte containing 35 g/L copper and 165 g/L sulfuric acid. Line represents the line of best fit.

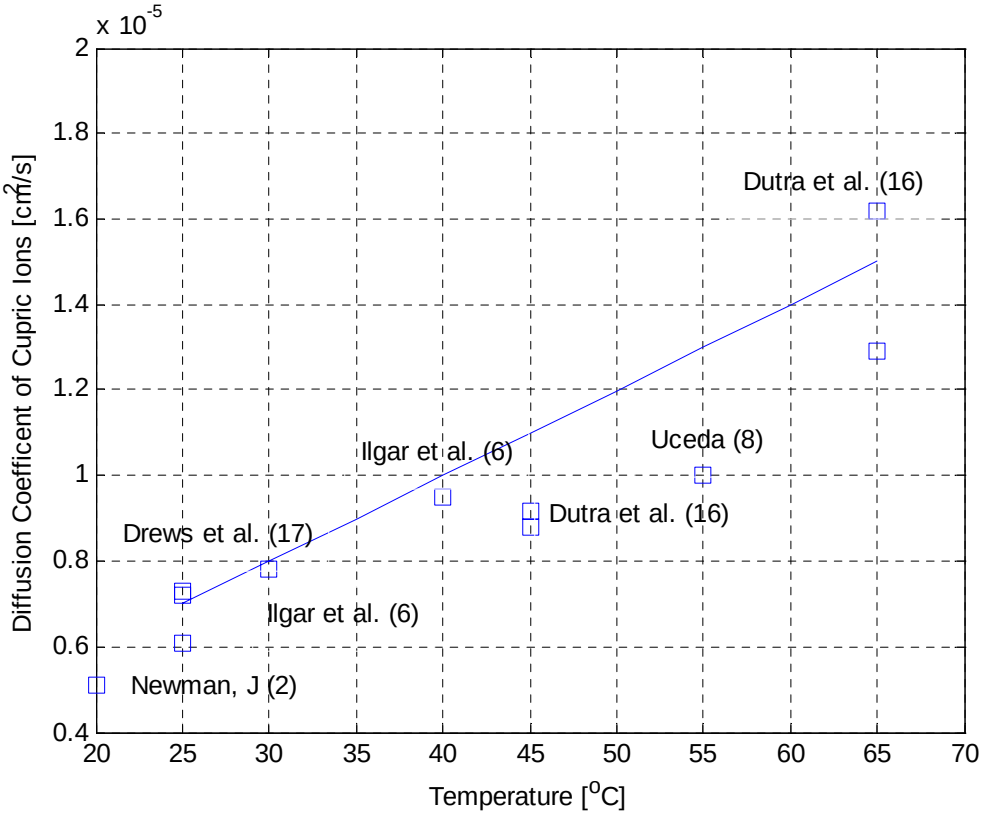

Figure 3-19: Variation of Diffusion Coefficient of Cupric Ions as a Function of Temperature

Legend: □ = original data from the literature stated in Appendix A and line = linear fitting.

Table 3-5: Effect of RPM and Temperature on Diffusion Layer Thickness

RPM	Temperature	Calculated		Experimental	
	°C	i_L, A/m^2	δ, µm	i_L, A/m^2	δ, µm
0	45	--	--	1037	97
0	65	--	--	1432	115
10	45	1070	94	1118	90
10	65	1655	99	1497	110
25	45	2032	49	1155	87
25	65	3143	52	1666	99

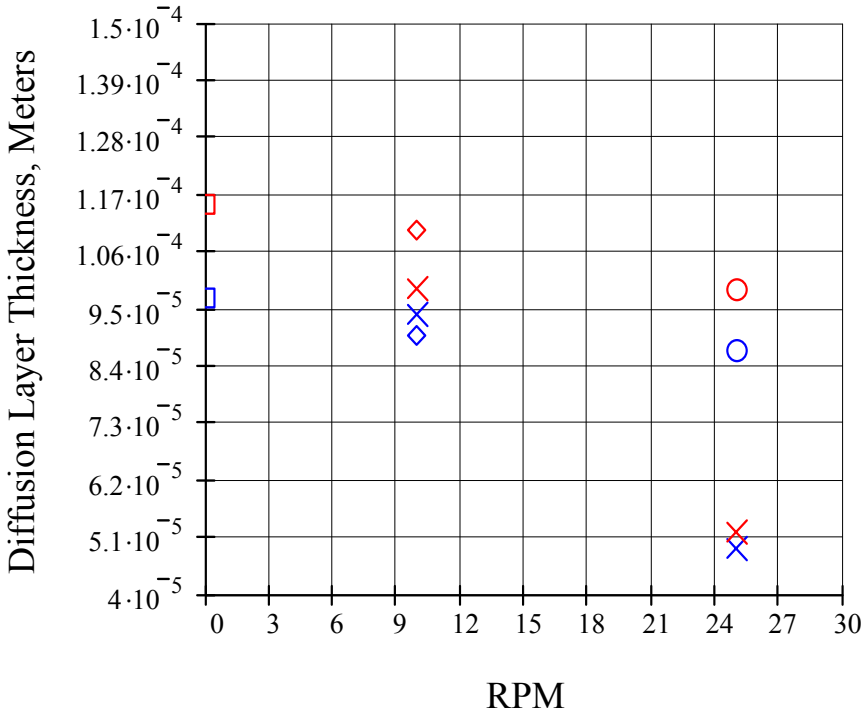

Figure 3-20: Effect of RPM on Calculated and Experimental Diffusion Layer Thickness at 45°C and 65°C

Legend: blue=45°C; red=65°C; x=Calculated using Arvia et al.'s LCD Equation; □= Experimental Free Convection; ◊ = Experimental at 10 rpm and o = Experimental at 25 rpm

The experimental diffusion layer thicknesses are greater at 0rpm, followed by 10rpm and 25rpm as expected. It is important to note that Arvia et al.'s[13] equation is more relevant for turbulent flow than for laminar flow with 2-3 vortexes, the flow regime in this thesis, and for temperatures from 16°C to 37°C. Therefore the discrepancy between the experimental and calculated values at 65°C in Table 3-20 is less significant.

3.2.4 Effect of Fluid Flow on Surface Roughness of Electrowon Copper

Preliminary tests were conducted to evaluate the rotating cylinder electrode by comparing results produced with those of Ilgar and O'Keefe[6] since the electrolyte compositions used in both works are similar as shown in Table 3-6. Minor differences between both electrolyte compositions occur in the sulfuric acid and chloride ions concentrations. This electrolyte composition for this thesis closely resembles that used in commercial practice. The number of coulombs per square centimetre applied in this testwork also closely replicates Ilgar and O'Keefe[6] data. The electrolyte composition shown in Table 3-6 was used throughout the testwork for this thesis.

Table 3-6: Electrolyte Composition and Other Variables

	This work	Ilgar and O'Keefe[6]
Copper, g/L	36	36
Sulfuric acid, g/L	160	150
Chloride ions, mg/L	25	20
Active cathode surface area, cm^2	27.91	12
Electrolyte volume per test, L	3.75	0.2
Inter-electrode distance, mm	40	30

Ilgar and O'Keefe[6] used this electrolyte composition to study the effect of chloride ions on the copper cathode surface roughness.

3.2.5 Experimental Results

Table 3-7 presents the results of the effect of the RCE rotation rate on surface roughness and these results are compared with those obtained by Ilgar and O'Keefe[6] in the absence of organic additives. The diffusion layer thickness reported in Table 3-7 was derived from Figure 3-20 above.

It can be seen in Table 3-7 that the measurement of average surface roughness obtained in this testwork is consistent with those results obtained with Ilgar and O'Keefe[6] given the differences in experimental design, temperature and electrolyte

composition. The effect of the minor differences in the electrolyte composition, the number of Coulombs applied and temperature are difficult to assess independently. The δ of 175μm at 30°C and 40°C for natural convection reported by Ilgar and O'Keefe[6] shown in Table 3-7 is about twice higher than the δ of 97μm at 45°C and 115μm at 65°C δ obtained at 0rpm (natural convection) for this thesis, shown in Table 3-5. However, these experimental δ values obtained for natural convection in this thesis more closely agrees with Drews et al.[17] who conducted Monte Carlo simulation using 78μm[4] for natural convection at 25°C. The δ presented in this thesis is below the average between δ values presented by Ilgar and O'Keefe[6] and Drews et al[17]. It could be therefore assumed that δ values determined in this thesis for 10 and 25 rpm agree with the above references.

Table 3-7: Effect of Diffusion Layer Thickness on Surface Roughness

	Ilgar and O'Keefe[6]		This study	
Electrowinning Cell Type	Parallel Plate Electrode		RCE	RCE
RCE rpm			25	10
Reynolds Number			225	90
Diffusion L. Thickness, μm	65	175*	88	94
Electrowinning Time, Hrs	5.5 or 4	5.5 or 4	4	4
Current Density, mA/cm^2	25 and 35	25 and 35	30	30
Temperature, °C	30 and 40	30 and 40	50	50
Coulombs, C/cm^2	500	500	434	434
Number of Fine Needles	N.A.**	N.A.**	None	50
Surface Roughness, Ra, μm	3.9±0.50	6.4-12.5±0.50	4.31±0.16	5.51±0.41

*Natural convection; **Not reported

The δ value of 65μm reported by Ilgar and O'Keefe[6] for highly stirred solutions agrees with the δ value of 94μm at 25rpm obtained *experimentally* in this thesis. The surface roughness reported by Ilgar and O'Keefe[6] accords with those measured in this thesis. Accordingly, it was possible to compare the results obtained in this thesis on the RCE with those of Ilgar and O'Keefe[6] on a parallel plate electrode assembly.

3.3 Effect of Polyacrylamide Preparation Media on Surface Roughness of Electrowon Copper

3.3.1 Introduction

It will be recalled that Mt. Gordon produced unusually smooth copper deposits and that it was suggested that it was caused by the presence of adventitious PAM. Therefore, the effect of polyacrylamide preparation in both mild alkaline and acidic solutions on the copper deposit surface roughness obtained from electrowinning tests was evaluated in the following Sections. It also compares the new additive derived from polyacrylamide with polyacrylic acid.

3.3.2 Experimental Conditions

Since PAM is known to undergo both acid and alkaline hydrolysis discussed in Section 2.6.2, a set of experiments were undertaken in which the acidity or alkalinity of PAM solution were systematically varied to see any difference in the surface roughness of copper electrowon under controlled conditions.

The preparation media for acid solutions was conducted by systematically halving the 160 g/L sulfuric acid concentration in the electrolyte. Therefore, polyacrylamide was prepared in full-strength electrolyte (160), 80, 40, 20 and 10 g/L sulfuric acid. The initial copper (36g/L) and chloride ions (25mg/L) concentrations were also halved in the same manner giving 2.25g/L and 1.56 mg/L, respectively in the last dilution. Polyacrylamide was also prepared in distilled water.

The polyacrylamide was also prepared in mildly alkaline aqueous solution. A maximum pH value of 8.5 was selected due to the impracticality of adding additional sodium hydroxide to the electrolyte of a commercial plant. At higher pH values than 8.5, sodium sulfate may unnecessarily increase the total sulfate ions in the electrolyte for copper electrorefining and therefore promote anode passivation. It can be seen in

Table 3-8 that polyacrylamide was prepared at pH value of 8.5 for Tests 1 and 2 at 50^{o}C and, for 3 and 2 hours, respectively.

The polyacrylamide (PAM) used was a high-molecular weight PAM i.e., 15 million Dalton Ciba Magnafloc® 800HP known as neutral or non-ionic PAM throughout this thesis. PAM was prepared in a 150mL glass long-necked beaker where 100mg PAM was weighed and then 100mL solution media added. This beaker sat in a thermostated water bath at 50^{o}C. Gentle stirring was applied through a 6cm height x 1.5cm diameter Teflon rod cut in a cross at one end to simulate an impeller. A 6mm diameter stainless steel shaft was inserted at the other end of the Teflon rod and to the stirrer. Therefore, the concentration of PAM in the preparation media was 1mg/mL. An Eppendorf pipette was used to dose 3.75mL of the polyacrylamide solution in 3.75L of electrolyte held at constant temperature in another water bath to achieve a final concentration of 1mg/L. The polyacrylamide once prepared was named "activated polyacrylamide" (APAM).

3.4 Experimental Results on the Effect of Polyacrylamide Preparation Media on Surface Roughness of Electrowon Copper

The experiments were designed to detect the effect of hydrolysis of polyacrylamide on the surface roughness of electrowon copper. Therefore, these experiments indirectly evaluate the adsorption of the hydrolysed polyacrylamide onto the stainless steel substrate and copper metal during the electrodeposition process. Some tests were replicated 2, 3 or 4 times to assess the hydrolysis conditions presented in the literature and thus to validate the results of this study.

Table 3-8 presents the summary of the experimental conditions and results. The one-way ANOVA between groups was analysed using SPSS software (version 11, 2003). Figure 3-21 shows the error bar plot of the surface roughness of the copper deposits produced as a function of preparation media. The error bars show the 95% confidence interval (CI). Since 8 replicate measurements of each test sample were collected, the number of replicate tests can be determined by dividing N (at the bottom of the graph) by 8. Thus it can be seen that the electrowinning test with PAM prepared

in water (Test 3) was repeated three times and in full-strength electrolyte two times (Test 8) and in 4-fold diluted electrolyte (Test 6) two times.

Despite the variety of mechanisms that are proposed for the smoothening effect of additives[18], a consensus exists that adsorption of the additive on the substrate plays the determining role[19, 20]. It can then be inferred from the above results that the type of copolymer, random or block copolymer, degree of PAM hydrolysis and its molecular weight have a strong effect on adsorption on stainless steel and copper metal and therefore on surface roughness of the copper deposits.

Table 3-8: Effect of Polyacrylamide Preparation Media on Surface Roughness

Test No.	1	2	3	4	5	6	7	8
Sulfuric Acid Conc., g/L	alkaline		Water	10	20	40	80	160
No. of Replicates	1	1	3	4	1	2	1	2
pH Preparation Media	8.5	8.5	6	1.5	1.25	1.14	1	<1
APAM Preparation Temp., ^{o}C	50	50	25	50	50	50	50	50
APAM Preparation Time, Hrs	3	2	2	2	2	2	2	2
EW PAM/APAM Conc. mg/L	1	1	1	1	1	1	1	1
Electrowinning Time, Hrs	6	6	6	6	6	6	6	6
Electrode Voltage Drop, V	1.46	1.42	1.45	1.35	1.4	1.38	1.36	1.33
Current Density, mA/cm^2	30	30	30	30	30	30	30	30
Electrolyte Temperature, ^{o}C	50	50	50	50	50	50	50	50
RCE rpm	10	10	10	10	10	10	10	10
Surface Roughness, Ra µm	8.47	7.03	7.09	6.59	7.11	7.09	7.29	7.32
Ra Standard Deviation, µm	0.93	0.43	0.44	0.47	0.41	0.85	0.49	0.61
Test4 One-Way ANOVA Sig.*	0.00	0.54	0.04		0.32	0.11	0.06	0.00
Dendrites<0.1mm length	10	Nil	Nil	Nil	Nil	Nil	Nil	Nil
S. Steel spots<1x1mm	Nil	Nil	Nil	Nil	Nil	1	Nil	Nil

*One- way ANOVA significance for Test 4, Tuckey, HSD.

The APAM used in Test 4 was prepared with 16-fold diluted electrolyte (sulfuric acid, 10 g/L or pH 1.5; copper, 2.25g/L) and produced a surface with a significantly lower roughness (6.59 ± 0.47 µm) than PAM prepared in water, full-strength electrolyte and alkaline hydrolysis (3hours preparation time). In Table 3-8, the significance of the difference in surface roughness between each test and Test 4 is

presented. In acid solutions, the significantly different mean surface roughness sequentially increase as the concentration of sulfuric acid increases indicating the true effect of acid concentration on the hydrolysis of polyacrylamide.

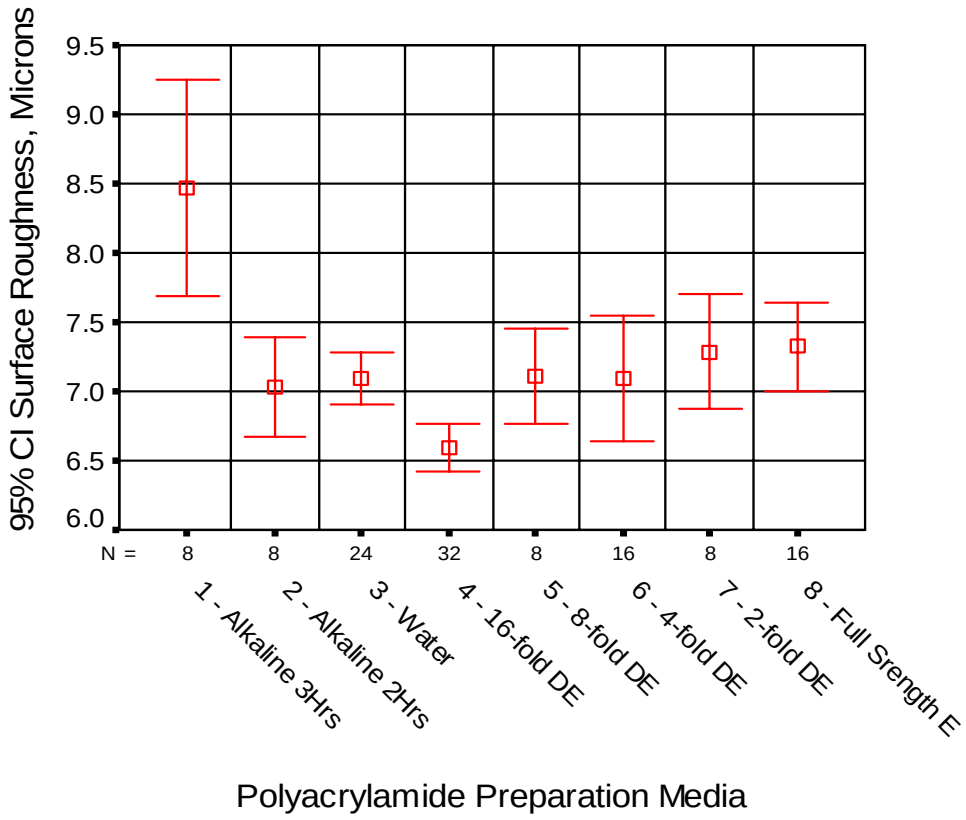

Figure 3-21: Error bar plot of the effect of preparation media on surface roughness of the copper deposits.

The average sequence length obtained from sequential mild alkaline hydrolysis followed by acid hydrolysis at pH 2 for 24 hours at 110^{o}C was 14[21] and this structure is known as a block copolymer. This suggest that PAM prepared for test 4 at a pH value of 1.5 also undergoes hydrolysis to form a block copolymer and cleavage in the backbone and therefore its 15million Dalton molecular weight was possibly also reduced due to the initial and fast acid hydrolysis reaction of PAM discussed in Section 3.2.1.2.

Grchev et al.[22] showed that surface coverage of 2-3mg/L polyacrylamide concentration in 0.5M sulfuric acid on gold and mild steel decreased from about 0.52 to 0.02 as the polyacrylamide molecular weight increased from 5x10^{3} to 1.5x10^{6} in the

temperature range from 20 to 80°C[22]. Because APAM preparation media influences surface roughness, it can be assumed that cleavage of the APAM backbone can occur and therefore the MW of APAM varies depending on the ageing of APAM in the electrolyte. Thus, the findings obtained from Test 4 can agree with the work of Grchev et al.[22]

The adsorption of polyacrylamide on gold and mild steel were explained in terms of substitutional absorption of the polymer on a bare metal surface followed by a significant desorption of water molecules from the surface[22]. Since surface roughness is directly related to adsorption, it is assumed that APAM prepared for Test 4 confers the highest adsorption.

Test 1 in which PAM was prepared at pH value of 8.5 at 50°C for 3 hours produced the highest surface roughness (8.47 ± 0.93 μm) compared with any test. Test 2 in which PAM was prepared at the same pH at 50°C for 2 hours gave a surface roughness of 7.03 ± 0.43 μm. It appears that under alkaline conditions surface roughness increases as PAM hydrolysis increases.

It was reported by Atkins[23] that at 50°C and 3 hours residence time the conversion of PAM into polyacrylic acid in alkaline solution was 61% while at 2 hours, this conversion was 31%. Surface roughness from hydrolysis of PAM in mildly alkaline solutions was the highest possibly due to the fast kinetics of polyacrylamide alkaline hydrolysis which suggests neighbouring-group catalysis superimposed on a general electrostatic effect[21, 24, 25]. These studies suggest that the rate constants for attack of an hydroxyl ion, OH^- at a polymer amide group with zero, one or two nearest-neighbour carboxylate groups exhibit relative rate constants $k_o > k_1, k_2$. Therefore, segments of acrylic acid functional groups are well distributed along the chain with an average sequence length of 1.4 from mild alkaline hydrolysis followed by strong alkaline hydrolysis[21] and this polymer structure is known as a random copolymer. Overall, the results obtained from Tests 1 and 2 from mild PAM hydrolysis are unlikely to be used in plant practice since it appears to produce a highly hydrolysed and random copolymer which is a detriment to the smoothness of the copper deposit.

In summary, it is assumed that that APAM undergoes cleavage in the backbone at 50^{o}C electrolyte temperature and block copolymers form at pH 1.5 which may also act as a small PAM molecular weight. These properties give PAM prepared for Test 4 the highest adsorption and therefore surface coverage than PAM prepared in water and full-strength electrolyte.

The polyacrylamide prepared in Test 4 is the discovery in this thesis and it is named "activated polyacrylamide" (APAM). This newly developed organic additive for copper electrowinning and possibly also for electrorefining will be compared with polyacrylic acid and Guar, the industry-standard additives, using electrowinning, Cyclic Voltammetry and Electrochemical Impedance Spectroscopy. .

3.4.1 NMR Analysis of Activated Polyacrylamide

Characterization of the activated polyacrylamide structure was determined by both ^{1}H and ^{13}C NMR spectroscopy in sulfuric acid and deuterium oxide (D_2O). All spectra were recorded on a Varian Mercury Console 300MHz spectrometer. ^{1}H spectra were obtained at 300MHz while ^{13}C spectra were obtained at 75 MHz. The NMR spectra were obtained using the polyacrylamide sample with about 15million Dalton molecular weight Ciba Magnafloc® 800HP *as received* from Mount Gordon Operations, Australia. Five wt% polyacrylamide was dissolved in 10g/L sulfuric acid and few drops of deuterium oxide (D_2O) at 50^{o}C for 2 hours in the absence of cupric ions. These conditions correspond to a solution of acid concentration similar to 16-fold diluted electrolyte (Test 4). Sonication was conducted for 30 minutes before NMR reading to obtain good quality spectra. Approximately 10^6 transients (over a weekend) were accumulated for the spectrum.

The raw data indicates that only the amide carbonyl carbon was detected in the 100-220ppm range and Figure 3-22 shows part of this section. Therefore it is suggested that carboxyl ions may be present only at relatively low concentrations, i.e., less than 10 mol %. Halverson et al.[21] and Feng et al.[26] reported ^{13}C NMR spectra for 10 mol % hydrolysed polyacrylamide and the relative intensity ratio of the amide carbonyl carbon to acid carbonyl carbon was about 6:1. This ratio decreases from about 5.25:2.3 to

3.5:2.5 for 22% and 33% hydrolysis, respectively. There must be acid carbonyl carbon present in APAM. Moreover, from the NMR spectra this is less than the instrument noise or least a 7:1 ratio. Had the acid carbonyl resonances exceeded approximately 10% of the amide carbonyl it would have been detected. The C^{13} NMR spectra presented in Figure 3-22 indicates that the proportional polyacrylamide hydrolysis must be less than 10%.

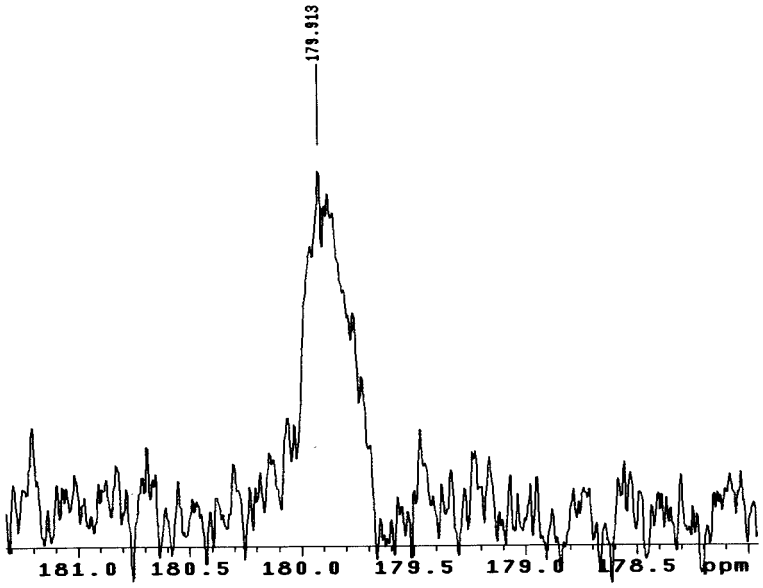

Figure 3-22: ^{13}C NMR signal intensity of activated polyacrylamide prepared in 10g/L sulfuric acid and deuterium oxide (D_2O) solutions at 50°C for 2 hours.

3.5 Effect of Activated Polyacrylamide Ageing on Surface Roughness

Tests were undertaken to determine the effect of ageing APAM in 16-fold diluted electrolyte (DE) and in full-strength electrolyte. The study in full-strength electrolyte was designed to estimate the effect of in-situ APAM hydrolysis in the electrowinning cells. Tests were also undertaken to verify the effect of ageing of APAM in 16-fold DE at room temperature for over 24 hours. This experiment was designed to determine if APAM could be stored prior to use. This test was also designed to verify whether an additional ageing in the electrolyte at 50°C following the

24-hours in 16-fold diluted electrolyte at 25°C could reduce surface roughness due to "as a matter of course" hydrolysis. Therefore, Test 1 was run with fresh APAM. Test 2 was run with APAM aged for 24 hours at 25°C in 16-fold DE. The electrolyte bath from Test 2 was maintained at 50°C for 24 hours and then Test 3 was run without adding any fresh APAM. Table 3-9 and Figure 3-23 show the results for this testwork.

Table 3-9: Effect of APAM Degradation in 16-fold DE and Full-Strength Electrolyte

Test No.	1	2	3
Number of Tests	1	1	1
pH Preparation Media	1.5	1.5	1.5
Preparation Temperature, oC	50	25	50
Residence Time in 16-fold DE, Hours	2	24	24
Residence Time in Electrolyte, Hours	0	0	24
Sulfuric Acid Concentration, g/L	10	10	10 & 160
APAM Conc. in Electrolyte, mg/L	1	1	1
Electrowinning Time, Hours	6	6	6
Electrode Voltage Drop, V	1.34	1.39	1.41
Current Density, mA/cm^2	30	30	30
Electrolyte Temp., °C	50	50	50
Diffusion Layer Thickness, µm (10rpm)	140	140	140
Surface Roughness, Ra µm	6.23	6.89	7.46
Ra Standard Dev., µm	0.41	0.68	0.86
Peaks per Centimetre	82.63	78.13	77.75
Peaks-per-Centimeter Std. Dev.	10.6	9.61	9.90
Dendrites Formation	Nil	Nil	Nil

Test 1 showed the lowest surface roughness with 2 hours prepared PAM in 16-fold diluted electrolyte followed by Test 2 with 24 hours residence time in 16-fold diluted electrolyte at 25°C. The surface roughness produced from Test 3 was the highest and indicated that an additional hydrolysis in the electrolyte at 50°C for 24 hours after 24 hours degradation in 16-fold diluted electrolyte at 25°C, increased surface roughness. Additional ageing or hydrolysis in the electrolyte increases the surface roughness possibly due to the decomposition of the active species, and/or formation of less adsorbent copolymers, such as imides.

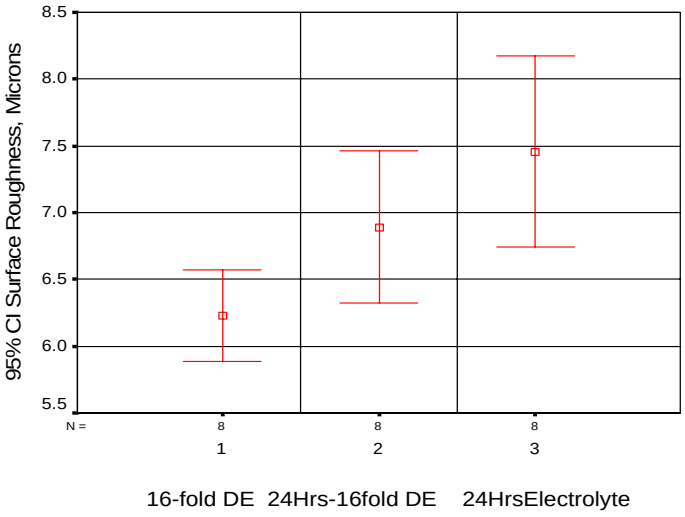

Figure 3-23: Degradation of Polyacrylamide in 16-fold Diluted Electrolyte and Full-Strength Electrolyte

Tests 1 and 2 are not statistically different indicating that APAM could be prepared for up to 24 hours without affecting significantly the surface roughness. However, based on the data shown in Figure 3-23, it may be better to prepare it every 12 or 6 hours and continuously dosed.

3.6 Comparison of Polyacrylic Acid and Activated Polyacrylamide

3.6.1 Introduction

The United States Patent 5,733,429 in the name of S. Martin and N. Nebeker[27] described the use of polyacrylic acid (repeating polymeric units having the structural formula of $-(CH_2\text{-}CH(COOX)\text{-}CH_2)_n$- wherein X=H, periodic table group 1 or group 2 element salts, an ammonium salt or mixture thereof) as an organic additive for copper electrowinning. US Patent 5,733,429 discusses the formation of dendrites or surface nodes on the cathodes and the increased potential to short-circuit the cell. The patent also claims that the use of polyacrylic acids, alone, prevent the formation of dendrites, minimizes anode flaking and prevents shorts in the circuit. The disadvantage with the process as described in US Patent 5,733,429 is that the preferred concentration of polyacrylic acid in electrolyte is between 10 and 200 mg/L. Such a high level of

dissolved organic material in electrolyte is known to cause significant carbon and hydrogen contamination of the copper cathode[28] when animal glue and thiourea are also used as additives.

Electrowinning tests were carried out to determine the comparative effectiveness of polyacrylic acid (PAA) and polyacrylamide prepared in 16-fold diluted electrolyte at 50^{o}C for 2 hours under stirring (APAM). This work was undertaken to compare the efficiency of APAM with PAA in minimizing the surface roughness of electrowon copper. The effectiveness of these organic additives in copper electrowinning was determined by directly measuring the surface roughness of the copper deposit. A high measurement of surface roughness would be indicative of a low effectiveness of the organic additive.

3.6.2 Comparison of Polyacrylic Acid and Activated Polyacrylamide in 4 Hour Electrowinning Test

Unless otherwise stated, polyacrylamide was dissolved in 16-fold diluted synthetic electrolyte (sulfuric acid, 10 g/L; copper, 2.25 g/L after dilution). PAA was prepared in a solution of sodium hydroxide at pH 11.5 at 50^{o}C of a concentration of 1000 mg/L for 2 hours.

Tests were undertaken to study the extent to which the efficacy of these two additives changed when held in full-strength electrolyte under plant conditions. Over a 12-hour test period, EW was undertaken for the first and last 4-hours. In the intermediate time (4-hours), the electrolyte temperature was kept constant at 50^{o}C. The first tests were carried out just after the 2-hours preparation at 50^{o}C at a pH 11.5 in sodium hydroxide for PAA and in 16-fold diluted electrolyte (i.e., 10 g/L H_2SO_4) for APAM. The results are presented in Table 3-10.

These experiments demonstrate that PAA consistently produced higher surface roughness than APAM. Moreover, PAA lost its efficacy at a much greater rate than APAM. It is noteworthy that APAM maintains its ability to produce smooth copper deposit over a period of at least 12-hours under conditions typical of contemporary

electrowinning and electrorefining plants. This has important practical benefits as it minimizes the dosing rate of the organic additive.

Table 3-10: Surface Roughness Using Polyacrylic Acid and Activated Polyacrylamide

	Polyacrylic Acid		**APAM**	
EW Test	0-4 Hrs	8-12 Hrs	0-4 Hrs	8-12 Hrs
Test No.	80A	80B	79A	79B
PAA/PAM Prep. Res. Time, Hrs	2	2	2	2
PAA/APAM Conc., mg/L	1	1	1	1
Electrowinning Time, Hours	4	4	4	4
Current Density, mA/cm^2	30	30	30	30
Electrolyte Temperature, ^oC	50	50	50	50
RCE rpm	10	10	10	10
Dendrite Observation	None	None	None	None
Surface Roughness, Ra, μm	5.70±0.20	7.78±1.20	5.06±0.52	5.50±0.66

3.6.3. Comparison of Polyacrylic Acid and Activated Polyacrylamide in 12-Hours Continuous Electrowinning

A continuous electrowinning test was conducted over a period of 12 hours continuous to further compare the effectiveness of APAM over PAA. A concentration of 10 mg/L was selected as described by Martin et al.[27] and for the purposes of comparison, both APAM and PAA were dosed at the same concentration. Table 3-11 summarises the results of this comparison.

Table 3-11 indicates that it was not possible to measure the surface roughness of the copper deposit produced by polyacrylic acid due to the presence of fine dendritic needles stopping the travel of the stylus tip. Qualitatively, the copper deposit produced by PAA was rougher compared to the copper deposit produced using APAM. Table 3-11 clearly shows that over 12-hours EW time, APAM is more effective at eliminating dendrite formations than polyacrylic acid.

Table 3-11: Comparison of PAA and APAM in 12 Hours Continuous EW

	Polyacrylic Acid	Activated PAM
Test No.	84	85
PAA/APAM Prep. Residence Time, Hrs	2	2
Concentration of PAA or APAM, mg/L	10	10
EW Time, Hrs	12	12
Current Density, mA/cm^2	30	30
Electrolyte Temperature, ^oC	50	50
RCE RPM	10	10
Dendrite	Numerous	None
Surface Roughness, Ra, μm	>20	10.5±1.

3.7 Discussion and Conclusions

It has been shown that the surface roughness obtained with the RCE built for this project agrees with the results obtained by Ilgar and O'Keefe[6] in the absence of organic additives.

It was therefore concluded that the use of the RCE for the testwork observed in this thesis would provide results consistent with those described in the literature. It appears that the use of surface roughness measurements to study the effect of organic additives under simulated commercial electrowinning and electrorefining conditions presented in this project thesis is the first of its kind. From this work, the following conclusions are drawn:

Despite the variety of mechanisms proposed for the smoothening effect of additives[18], a consensus exists that *adsorption* of the additive on the substrate plays the determining role[19, 20]. It is then be inferred from the results in this Chapter that the type of copolymer, random or block copolymer, degree of PAM hydrolysis and its molecular weight have a strong effect on adsorption on stainless steel and copper metal and therefore on surface roughness of the copper deposits.

It was shown that when 15 million MW polyacrylamide was prepared in 16-fold diluted electrolyte at 50^{o}C for 2-hours the surface roughness of the copper deposit was statistically lower than when PAM was either prepared in water, where hydrolysis is

insignificant, full-strength electrolyte or alkaline solution at pH 8.5 (3 hours preparation time).

Halverson et al.[21] showed that PAM dissolved at pH 2 for 24 hours at 110^{o}C was 57% hydrolysed to form a block copolymer with a polyacrylic acid sequence length of 14. In this work, NMR data suggests that polyacrylamide prepared for Test 4 at pH equal to 1.5 at 50^{o}C under stirring for 2-hours was less than 10% hydrolysed. These data are mutually consistent since the experimental hydrolysis at 110^{o}C in 24-hours would be much greater than that observed at 50^{o}C for 2-hours. It is therefore assumed that the APAM produced in this work is a block copolymer as described schematically below:

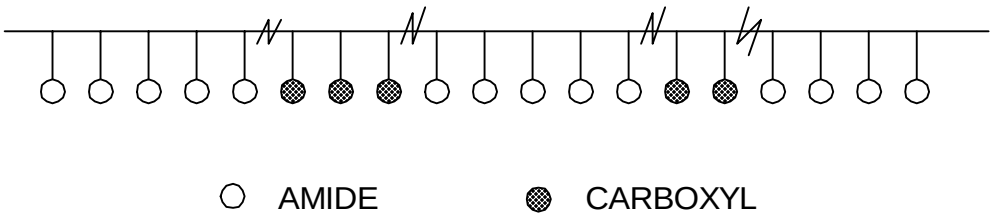

PAM prepared in water, where hydrolysis is insignificant, and in full-strength electrolyte produces similar hydrolysis reactions and products. These hydrolysis products may adsorb statistically less than the APAM possibly due to polyacrylimide formation discussed in Chapter 2.

Grchev et al.[22] showed that surface coverage of 2-3mg/L polyacrylamide concentration in 0.5M sulfuric acid on gold and mild steel decreased from about 0.52 to 0.02 as the polyacrylamide molecular weight increased from 5x103 to 1.5x106 in the temperature range from 20 to 80oC. Because APAM preparation media influences surface roughness, it can be assumed that cleavage of the APAM backbone can occur and therefore the MW of APAM varies depending on the ageing of APAM in the electrolyte. Thus, the findings obtained with APAM can agree with the work of Grchev et al.[22]

Since surface roughness is directly related to adsorption, APAM prepared in 16-fold electrolyte at 50^{o}C and under stirring for 2-hours gives the highest adsorption and

therefore surface coverage than PAM prepared in water and full-strength electrolyte. The adsorption mechanism of APAM appears to conform to partially hydrolysed block copolymer through hydrogen and covalent bonding as discussed in Chapter 2.

PAM hydrolysed in alkaline media is much less effective than 'APAM'. Therefore, based on these results and literature[21, 24, 25] the hydrolysis product in alkaline solutions is a random copolymer as schematically described below:

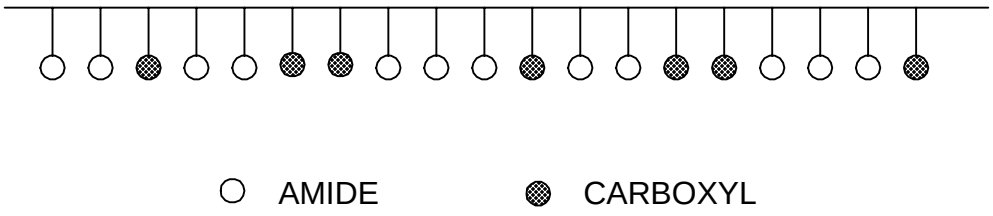

APAM is more effective at eliminating dendrite formations than polyacrylic acid up to 12 hours electrowinning. APAM can be maintained in 16-fold diluted electrolyte without significantly affecting surface roughness.

3.8 References

1. Baker DR, Verbrugge MW, Newman J. *A Transformation for the Treatment of Diffusion and Migration. Application to the Simulation of Electrodeposition onto Microelectrode Geometries*. Proceedings - Electrochemical Society 1992;92-3(Proc. Int. Symp. Electrochem. Microfabr., 1st, 1991):279-90.

2. Newman J, Thomas-Alyea KE. *Electrochemical Systems*. Third ed. Hoboken, New Jersey: John Wiley & Sons, Inc.; 2004.

3. Barkey D, Muller R, Tobias C. *Roughness Development in Metal Electrodeposition I. Experimental Results*. Journal of the Electrochemical Society 1989;138(8):2199-2207.

4. Wilke C, Eisenberg M, Tobias C. *Correlation of Limiting Currents under Free Convection Conditions*. J. Electrochem. Soc. 1953;100(11):513-523.

5. Landau U. Determination of Laminar and Turbulent Mass Transport Rates in Flow Cells by the Limiting Current Technique. In: *Lectures in Electrochemical Engineering*: The American Institute of Chemical Engineers; 1981. p. 75-87.

6. Ilgar E, O'Keefe T. Surface Roughening of Electrowon Copper in the Presence of Chloride Ions. In: Dreisinger D, editor. *Aqueous Electrotechnologies: Progress in Theory and Practice*; 1997: The Minerals Metals and Materials Society; 1997. p. 51-62.

7. Ettel V, Tilak B, AS G. *Measurement of Cathode Mass Transfer Coefficients in Electrowinning Cells*. J. Electrochem. Soc. 1974;121(7):867-872.

8. Uceda D. Determination of Mass Transfer Characteristics in the Electrolysis of Copper [PhD Thesis]. Missouri-Rolla: University Missouri-Rolla; 1988.

9. Obretenov W, Schmidt U, Lorenz W, Staikov G, Budevski E, Carnal D, Muller U, Siegenthaler H, Schmidt E. *Underpotential Deposition and Electrocrystallization of Metals*. J. Electrochem. Soc. 1993;140(3):692-703.

10. Budevski E, Staikov G, Lorenz W. *Electrochemical Phase Formation and Growth, an Introduction to the Initial Stages of Metal Deposition*. New York: VCH; 1996.

11. Schmidt W. In Situ Studies of Copper Electrodeposition in the Presence of Organic Additives Using Atomic Force Microscopy [PhD]. Urbana-Champaign: University of Illinois; 1996.

12. Eisenberg M, Tobias C, Wilke C. *Ionic Mass Transfer and Concentration Polarization at Rotating Electrodes*. Journal of the Electrochemical Society 1954;101(6):306-319.

13. Arvia AJ, Carrozza JSW. *Mass Transfer in the Electrolysis of Cuso4-H2so4 in Aqueous Solutions under Limiting Current and Forced Convection Employing a Cylindrical Cell with Rotating Electrodes*. Electrochimica Acta 1962;7:65-78.

14. Manzanares JA, Kontturi K. Diffusion and Migration. In: Calvo EJ, editor. *Interfacial Kinetics and Mass Transport*: Wiley-VCH; 2003. p. 81-121.

15. Price D, Davenport W. *Physico-Chemical Properties of Copper Electrorefining and Electrowinning Electrolytes*. Metallurgical & Materials Transactions B-Process Metallurgy & Materials Processing Science 1981;12B:639-643.

16. Dutra A, O'Keefe T. *Copper Nucleation on Titanium for Thin Film Applications*. Journal of Applied Electrochemistry 1999;29:1217-1227.

17. Drews T, Ganley J, Alkire R. *Evolution of Surface Roughness During Copper Electrodepositon in the Presence of Additives*. J. Electrochem. Soc. 2003;150(5):C325-C334.

18. Onicio L, Muresan L. *Some Fundamental Aspects of Levelling and Brightening in Metal Electrodeposition*. Journal of Applied Electrochemistry 1991;21:565-574.

19. Jordan K, Tobias C. *The Effect of Inhibitor Transport on Leveling in Electrodeposition*. J. Electrochem. Soc. 1991;138(5):1251-1259.

20. Chung D. Localized Adsorption of Organic Additives During Copper Electrodeposition [Ph.D.]. Urbana-Champaign: University of Illinois; 1996.

21. Halverson F, Lancaster J, O'Connor M. *Sequence Distribution of Carboxyl Groups in Hydrolyzed Polyacrylamide*. Macromolecules 1985;18(6):1139-44.

22. Grchev T, Cvetkovska M, Stafilov T, Schultze J. *Adsorption of Polyacrylamide on Gold and Iron from Acidic Aqueous Solutions*. Electrochimica Acta 1991;36(8):1315-1323.

23. Atkins M, Biggin I, Kidd D; inventors. BP Chemicals Limited, assignee. Hydrolysis of Polymers. United States patent 5,081,195. 1992 January 14, 1992.

24. Panzer H, Halverson F, Lancaster J. *Carboxyl Sequence Distribution in Hydrolyzed Polyacrylamide*. Polymeric Materials Science and Engineering 1984;51:268-71.

25. Panzer H, Halverson F. Blockiness in Hydrolyzed Polyacrylamide. In: Moudgil B, Scheiner B, editors. *Flocculation Dewatering, Proc. Eng. Found. Conf.*; 1988; Palm Coast Florida, USA; 1988. p. 239-49.

26. Feng Y, Billon L, Grassl B, Khoukh A, Francois J. *Hydrophobically Associating Polyacrylamides and Their Partially Hydrolyzed Derivatives Prepared by Post-*

Modification. 1. Synthesis and Characterization. Polymer 2002;43(7):2055-2064.

27. Martin S, Nebeker N; inventors. Enthone-OMI, Inc, assignee. Polyacrylic Acid Additives for Copper Electrorefining and Electrowinning. United States patent 5,733,429. 1998.

28. Chia D, Patel G. *Copper Rod and Cathode Quality as Affected by Hydrogen and Organic Additives*. Wire Journal International 1992(Nov.):67-75.